國立臺灣大學理學院物理學研究所

碩士論文

Graduate Institute of Physics

College of Science

National Taiwan University

Master's Thesis

具有手性對稱性及具有反射對稱性的 (1+1) 維電荷守恆系統的費米子對稱保護拓樸相

Fermionic Symmetry-Protected Topological Phases for (1+1)*d* Charge-conserved Systems with Chiral Symmetry and with Reflection Symmetry

李晨申

Chen-Shen Lee

指導教授: 謝長澤 博士

Advisor: Chang-Tse Hsieh Ph.D.

中華民國 113 年 1 月

January, 2024

doi:10.6342/NTU202400302

國立臺灣大學碩士學位論文

口試委員會審定書

具有手性對稱性及具有反射對稱性的 (1+1) 維電荷守恆系統的費米子對稱保護拓樸相

Fermionic Symmetry-Protected Topological Phases for (1+1)*d* Charge-conserved Systems with Chiral Symmetry and with Reflection Symmetry

本論文係李晨申君（R10222096）在國立臺灣大學物理學研究所完成之碩士學位論文，於民國 113 年 1 月 23 日承下列考試委員審查通過及口試及格，特此證明

口試委員：謝長澤

（指導教授）

張明哲

高賢忠

所　　長：理學院物理學系系主任張寶棣

Acknowledgements

在這項研究中，我要特別感謝我的指導教授，謝長澤教授。在一開始時，謝教授就以我過往經驗為基礎，明確地指出了一個合適的研究方向。謝教授還將我介紹給在京都大學的鹽崎謙教授認識，讓我能在研究過程中得到更多寶貴建議。非常感謝兩位教授讓我能順利完成這項研究。我也非常感謝帶我走進目前領域的引路人，高賢忠教授。此外，我也很感謝張明哲教授、游至仕教授及高英哲教授的教導，讓我能夠更好地理解凝態物理和拓樸學之間的關係。我還想感謝姚有徽學長，從大學開始，學長總是很有熱情的和我討論物理問題，也告訴了我很多研究上該注意的事，甚至有時還幫我打印資料。最後，我想感謝一直支持我的家人和讓我研究生涯更為充實的其他同學。

doi:10.6342/NTU202400302

摘要

本文旨在為受兩種不同對稱性保護的 (1+1) 維費米子對稱保護拓樸相提供物理解釋，其分別是 $U(1)$ 和手性對稱性及 $U(1)$ 和反射對稱性。

第一章提供了一些與對稱保護拓樸相相關知識的簡要回顧。除了對稱保護拓樸相的基本定義及分類它們的方法，我們還介紹了如何透過配邊理論建構多體拓樸不變量及體邊對應的概念。

在第二和第三章中，我們提出了一種能夠協助人們物理地理解這兩種 (1+1) 維費米子對稱保護拓樸相的方法，主要是透過建立它們對應的多體拓樸不變量及可分解系統之間的關係。其中，可分解系統是指系統在週期性邊界條件下可以被分解成某個子系統的多個副本。此外，我們還指出了有限尺寸效應在多體系統和自由費米子系統之間的不同。

第四章主要在探討平移對稱性如何改變這兩種 (1+1) 維費米子對稱保護拓樸相。同時，我們也為在考慮平移對稱性後產生的拓樸相建立對應的拓樸不變量。

關鍵字：對稱保護拓樸相、手性對稱性、反射對稱性、多體拓樸不變量、體邊界對應

doi:10.6342/NTU202400302

Abstract

This thesis aims to provide a physical interpretation of the (1+1)d fermionic symmetry-protected topological (SPT) phases protected by $U(1)$ and chiral ($U(1)+S$) symmetry and protected by $U(1)$ and reflection ($U(1)+R$) symmetry.

The first chapter contains some basic knowledge related to the SPT phases. Beyond the concept of SPT, we introduce the classification schemes of SPT phases, how to construct many-body topological invariants through the cobordism theory, and the idea of bulk-boundary correspondence.

In the second and third chapters, as an approach to physically understanding the (1+1)d fermionic SPT phases protected by $U(1)+S$ and $U(1)+R$, we construct the relations between their corresponding many-body topological invariants and the decomposable systems, defined as systems that can be decomposed into n copies of a subsystem under the consideration of periodic boundary conditions. Additionally, we indicate that the finite-size effect on many-body systems differs from that on free fermion systems.

The fourth chapter focuses on how translation symmetry changes two SPT phases studied in the previous two chapters. We also construct a set of topological invariants to

doi:10.6342/NTU202400302

describe the SPT phases that involve translation symmetry.

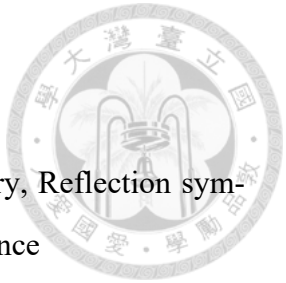

Keywords: Symmetry-protected topological phase, Chiral symmetry, Reflection symmetry, Many-body topological invariant, Bulk-boundary correspondence

doi:10.6342/NTU202400302

Contents

doi:10.6342/NTU202400302

doi:10.6342/NTU202400302

List of Figures

doi:10.6342/NTU202400302

doi:10.6342/NTU202400302

doi:10.6342/NTU202400302

List of Tables

doi:10.6342/NTU202400302

Chapter 1

Introduction

In this chapter, before diving into the (1+1)d fermionic symmetry-protected topological (SPT) phases protected by $U(1)$ and chiral symmetry and protected by $U(1)$ and reflection symmetry, we give a brief review of SPT phases and introduce some basic knowledge regarding classification schemes, topological invariants, and bulk-boundary correspondence.

1.1 Symmetry-Protected Topological Phases

Topological phases are gapped phases of matter that are not described by Landau symmetry-breaking theory but are separated by topological phase transitions, which can be gapless phases or quantum critical points. Specifically, in the thermodynamic limit, systems in a certain topological phase cannot adiabatically deform to trivial systems or systems in another topological phase without undergoing gapless phases or quantum critical points. One can generalize this idea and define symmetry-protected topological (SPT) phases [1, 2]. Without symmetry, SPT phases are topologically equivalent to trivial ones. However, they cannot be adiabatically connected to trivial phases without topological phase transitions while preserving certain symmetries. It's worth noting that SPT phases are different from symmetry-enriched topological (SET) [3, 4] phases. SET phases are topologically non-trivial even without symmetry.

doi:10.6342/NTU202400302

1.2 Classification of SPT phases

For free fermion systems, it's convention to describe them in the single-particle basis set. Assuming that systems have translation symmetry in each spatial direction, one can transform the single-particle Hamiltonians into Bloch Hamiltonians through Fourier transformation, describing systems in the momentum space. Therefore, it's sensible to classify free fermion SPT phases in momentum space. We have several schemes to address the classification problem of free fermions systems with on-site symmetry in momentum space, including the homotopy classification [5], which is under the consideration of the low-energy description of Bloch Hamiltonians near a certain momentum point, the vector bundle classification [6], and the K-theory classification [7, 8]. Among these, the most commonly used one is K-theory classification because this approach is a classification based on "stable equivalence", which guarantees that adding trivial atomic bands will not change the topological properties of SPT phases. Additionally, SPT phases can be protected by crystalline symmetry as well. One of the most systematic methods to study their classification is twisted equivariant K-theory [9, 10]. Beyond momentum space, one can classify free fermion SPT phases in real space [11], which will arrive at the same result as those classified in momentum space.

With the introduction of interaction, the many-body systems cannot be described in the single-particle basis set, so the classification schemes applied in the momentum space are invalid here. Unlike their free fermion counterparts where the corresponding classification is based on topological phase transition regarding band theory, the classification of interacting SPT phases is related to the ground states. In the language of quantum entanglement, the ground states of SPT phases can be considered as short-range entan-

doi:10.6342/NTU202400302

gled (SRE) states [12] with symmetry. In other words, the information on SPT phases is encoded in ground states, so we can classify SPT phases in terms of ground states. For interacting SPT phases protected by on-site symmetry, their classification problem can be systematically addressed by group (super)cohomology theory [13, 14], which produces topological actions of nonlinear σ models in discretized Euclidean spacetime. For the crystalline symmetry, there are two different ideas for classifying their SPT phases. One is related to topological quantum field theory [15]. By assuming the scale of systems is large enough compared with correlation length, we can regard crystalline symmetries as gauge fields. Hence, one can classify crystalline SPT phases by the method used for classifying SPT phases protected by on-site symmetry. The other idea is constructing SPT phases through "dimensional reduction" [16]. The most organized classification scheme concerning this idea is applying the Atiyah-Hirzeburch spectral sequence (AHSS) to the generalized homology theory [17].

Cobordism theory can be applied to classify interacting SPT phases as well [18–21]. Additionally, it can be used to formulate cobordism invariant partition functions that act as many-body topological invariants [22–24]. It's worth noting that the applicability of this classification scheme is still a conjecture because there is no relativistic symmetry in condensed matter physics, but the cobordism classification of fermionic SPT phases is given by cobordism groups equipped with pin or spin structure, which implies the existence of relativistic symmetry. However, even if there is an issue regarding relativistic symmetry, the classification based on cobordism theory surprisingly remains applicable. Especially, when we employ other schemes to classify interacting SPT phases, including bosonic and fermionic ones, we will get the same result as those derived from cobordism theory.

doi:10.6342/NTU202400302

1.3 Many-body topological invariants

Topological invariants can be utilized to detect the SPT phases of matter. For instance, the winding number can detect the (1+1)d free fermion SPT phases protected by chiral symmetry. The exploration of topological invariants regarding free fermion systems is almost full-fledged (see [25] and references therein). However, in the interacting scope, the discovery of topological invariants is still so limited. One of the methods to construct many-body topological invariants is based on the Euclidean path integral combined with the cobordism theory [22–24]. To be more specific, in the operator formalism, SPT phases can be characterized by the non-local order parameters, so it is reasonable to construct the many-body topological invariants by encoding the order parameters in a path integral, which leads to

$$Z(X,\eta,A)=\int\prod_i D\phi_i\,\exp[-S(X,\eta,A,\phi_i)]. \tag{1.1}$$

Here, ϕ_i is the matter field, X is the Euclidean spacetime, and the above path integral represents integrating over all matter degrees of freedom of the system for a given background (X,η,A). If we consider a unitary on-site symmetry G, we can introduce the background G gauge field A, which couples to the matter fields. Note that for a global symmetry $\tilde{G}$, it is conventional to decompose $\tilde{G}$ into two parts. One part consists of unitary on-site symmetries and another part includes symmetry transformations that reverse the orientation of spacetime manifolds. η is the additional data, such as the spin structure for fermionic systems. For the invertible gapped phases where the ground state is unique on all spatial manifolds, including SPT phases, this partition function is expected to have a topological part, which is a $U(1)$ phase and independent of local data. To put it differently, the topo-

doi:10.6342/NTU202400302

logical part of $Z(X,\eta,A)$ defines a topological quantum field theory (TQFT). Because our object is to establish the connection between $Z(X,\eta,A)$ and the SPT phases, a proper choice of background (X,η,A) is necessary. People find that the cobordism theory can address the problem regarding how to choose (X,η,A) properly [21], Hence, by use of the ground state and symmetry transformations, the (cobordism invariant) partition function $Z(X,\eta,A)$ on the generating manifold, which is the generator of the cobordism group, can serve as the many-body topological invariant [22–24]. Note that the above statement implies that the classification of SPT phases can be characterized by $\mathrm{Arg}[Z(X,\eta,A)]$.

In the rest of this section, we will introduce the many-body topological invariants used to detect the SPT phases we focus on, the (1+1)d fermionic SPT phases protected by $U(1)$ and chiral ($U(1)+S$) symmetry and protected by $U(1)$ and reflection ($U(1)+R$) symmetry.

1.3.1 Chiral-respecting topological invariant

The above idea allows us to construct the many-body topological invariant for (1+1)d fermionic systems with $U(1)+S$ symmetry. Since the corresponding classification is given by the cobordism group $\Omega_2^{\mathrm{pin}^c}(pt)=\mathbb{Z}_4$ that is generated by real projective plane $\mathbb{R}P^2$, the topological invariant here is the partition function (1.1) on $\mathbb{R}P^2$, which can be constructed by using partial transpose and chiral transformation in the operator formalism [24], as

$$Z^S=\mathrm{Tr}_I[\rho_I U_S^{I_1}\rho_I^{T_1}[U_S^{I_1}]^\dagger], \tag{1.2}$$

doi:10.6342/NTU202400302

where ρ_I is the reduced density matrix, $\rho_I^{T_1}$ is the partial transpose of ρ_I, and $U_S^{I_1}$ is the unitary part of chiral symmetry. To proceed, we would like to elaborate on how to evaluate Z^S. First, consider a (1+1)d fermionic system with periodic boundary conditions (PBCs), and then introduce an interval $I = I_1 \cup I_2$ on this closed chain S^1. Here, $I = \{c_i, ..., c_n\} \subset S^1$, and $I_1 \cup I_2 = \{c_i, ..., c_j\} \cup \{c_{j+1}, ..., c_n\}$, where c_j is the complex fermion at lattice site j. For a given ground state $|GS\rangle$, ρ_I can be obtained by tracing out the degrees of freedom outside I, $\rho_I = \mathrm{Tr}_{S^1 \setminus I}[|GS\rangle \langle GS|]$. Given that ρ_I can be expanded by the occupation number basis, $\rho_I = \sum_{n,\overline{n}} a_{n,\overline{n}} |n\rangle \langle \overline{n}| = \sum_{n,\overline{n}} a_{n,\overline{n}} |\{n_j\}_{j\in I_1}, \{n_j\}_{j\in I_2}\rangle \langle \{\overline{n}_j\}_{j\in I_1}, \{\overline{n}_j\}_{j\in I_2}|$, where $a_{n,\overline{n}}$ is a complex number, we can study the fermionic partial transpose combined with $U_S^{I_1}$ in the occupation number basis, which is given by

$$\begin{aligned} &U_S^{I_1}(|\{n_j\}_{j\in I_1}, \{n_j\}_{j\in I_2}\rangle \langle \{\overline{n}_j\}_{j\in I_1}, \{\overline{n}_j\}_{j\in I_2}|)^{T_1}[U_S^{I_1}] \\ &= c_S U_S^{I_1} C_f^{I_1}(|\{\overline{n}_j\}_{j\in I_1}, \{n_j\}_{j\in I_2}\rangle \langle \{n_j\}_{j\in I_1}, \{\overline{n}_j\}_{j\in I_2}|)^{T_1}[C_f^{I_1}]^\dagger [U_S^{I_1}]^\dagger, \end{aligned} \tag{1.3}$$

where $c_S = i^{[\tau_1+\overline{\tau}_1]}(-1)i^{(\tau_1+\overline{\tau}_1)(\tau_2+\overline{\tau}_2)}$ and

$$\tau_i = \sum_{j\in I_i} n_j, \quad \overline{\tau}_i = \sum_{j\in I_i} \overline{n}_j, \quad [\tau] = \begin{cases} 0 & (\tau : \text{even}) \\ 1 & (\tau : \text{odd}) \end{cases}, \quad C_f^{I_1} = \prod_{j\in I_1} (c_j^\dagger + c_j). \tag{1.4}$$

In this thesis, we employ cut and glue construction [26] to evaluate Z^S. Precisely, for all systems we study, Z^S can be evaluated by focusing on the 12 complex fermions at the boundary of the interval $I = I_1 \cup I_2$ only, such as

$$c_2 \ \ldots \ c_4 \ \ c_6 \ \ldots \ c_8 \ \ c_{10} \ldots \ c_{12}$$

$$\underbrace{c_1 \ \ldots \ c_3}_{I_1} \ \ \underbrace{c_5 \ \ldots \ c_7}_{I_2} \ \ c_9 \ \ \ldots \ c_{11}$$

doi:10.6342/NTU202400302

In other words, when calculating Z^S, we only consider systems with 4 complex fermions in I_1, I_2, and $S^1 \backslash I$ respectively. Notice that the boundary conditions here should be PBCs, so the fermions c_{11} and c_{12} are located next to the left boundary of I_1.

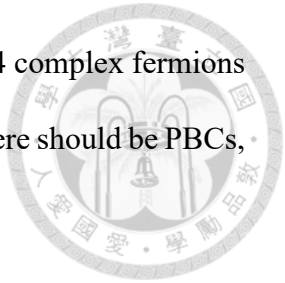

1.3.2 Reflection-respecting topological invariant

For (1+1)d fermionic systems with $U(1)+R$ symmetry, we have the same cobordism group $\Omega_2^{\text{pin}^c}(pt) = \mathbb{Z}_4$ as the chiral cases, so the corresponding classification is $\mathbb{Z}_4$ as well. Here, we can use the partial reflection to construct the topological invariant [23], as

$$Z^R = \langle GS | \, [U_\alpha R]_I \, | GS \rangle \,, \tag{1.5}$$

where $|GS\rangle$ is the ground state, and $[U_\alpha R]_I$ is the partial reflection. To explain these notations more clearly, we would like to illustrate how to evaluate Z^R. First, we consider a (1+1)d system with PBCs that respects the reflection symmetry $R c_j^\dagger R^{-1} = c_{N_{\text{tot}}-j+1}^\dagger$ and the $U(1)$ symmetry, where N_{tot} is the total number of sites, then we pick up an interval $I = \{c_a, \ldots, c_b\} \subset S^1$ ($a < b < N_{\text{tot}} \in \mathbb{Z}$) and define the partial reflection $[U_\alpha R]_I$

$$[U_\alpha R]_I c_j^\dagger ([U_\alpha R]_I)^{-1} = e^{-i\alpha} c_{b-j+a}^\dagger \quad [U_\alpha R]_I \, |0\rangle = |0\rangle \,, \quad j \in \{a, \ldots, b\}, \tag{1.6}$$

where the center of the interval I we pick is the same as the reflection center. To provide the $\mathbb{Z}_4$ classification, the appropriate $U(1)$ phase here is $\alpha = \pm\pi/2$. For all the cases we study later, we take $\alpha = -\pi/2$.

doi:10.6342/NTU202400302

1.4 Bulk-boundary correspondence

One of the reasons why people pay attention to topological phases is the existence of bulk-boundary correspondence, which relates the one-to-one relation between the bulk topological invariants and the non-trivial boundary phenomena [27–41]. For SPT phases, one renowned example that shows such correspondence is topological insulators [27–32] [1]. As a case in point, for (1+1)d free fermion systems with chiral symmetry, their number of zero-energy edge states is characterized by the winding number, which can be used to detect the corresponding SPT phases as well [25]. From this perspective, bulk-boundary correspondence can provide a physical interpretation of SPT phases and enable the SPT phase to be probed experimentally. In this thesis, we focus on how to physically realize (1+1)d fermionic SPT phases protected by $U(1)+S$ symmetry and protected by $U(1)+R$ symmetry. The essential ingredient behind our approaches to achieving it is bulk-boundary correspondence.

[1] Not all topological insulators are in the family of SPT phases. For instance, the Chern Insulator belongs to long-range-entangled phases, but it has an invertible topological order.

doi:10.6342/NTU202400302

Chapter 2

(1+1)d Fermionic SPT Phases Protected by $U(1)$ and Chiral Symmetry

Let's start with the definition of $U(1)$ symmetry and chiral symmetry S. A lattice Hamiltonian H is said to respect $U(1)$ symmetry if it remains invariant for the transformation $c_j \to e^{i\theta}c_j$ with $e^{i\theta}$ being the phase factor. For systems that respect chiral symmetry in this thesis, we have $SHS^{-1} = H$ with $Sc_jS^{-1} = (-1)^j c_j^\dagger$. The free fermion and fermionic SPT phases of (1+1)d systems with $U(1) + S$ symmetry are classified by $\mathbb{Z}$ and $\mathbb{Z}_4$ respectively. In this chapter, we will show how to physically realize this $\mathbb{Z}_4$ classification. Our approach to this is to find out the bulk-boundary correspondence between chiral-respecting topological invariants (1.2) and decomposable systems. If a system with PBCs can be decomposed into n copies of a subsystem with a unique ground state, we call the system a decomposable system. More precisely, in the language of the matrix product states, considering decomposable systems means that we discuss something within the limit of zero correlation length.

doi:10.6342/NTU202400302

2.1 Bulk-boundary correspondence in (1+1)d free fermion systems with $U(1)$ and chiral symmetry

One strategy to understand interacting SPT phases is generalizing bulk-edge correspondence in free fermion systems to interacting systems [42, 43]. Therefore, before discussing (1+1)d fermionic SPT phases protected by $U(1)+S$ symmetry, we give a brief review of their free fermion counterpart, with a particular focus on bulk-boundary correspondence. For free fermion systems, one can describe them in the single-particle basis set, yielding single-particle Hamiltonians $\hat{H}$. By assuming translation symmetry and then using Fourier transformation, we can transform $\hat{H}$ into the Bloch Hamiltonian $\mathscr{H}$. A free fermion system is said to respect chiral symmetry if there exists a unitary operator S, where

$$S\mathscr{H}(k)S^{-1} = -\mathscr{H}(k). \tag{2.1}$$

In the presence of chiral symmetry, the Hamiltonian can be brought into block-off diagonal form in the chiral basis, such as

$$\mathscr{H}(k) = \begin{pmatrix} 0 & D(k) \\ D^{\dagger}(k) & 0 \end{pmatrix}, \quad \text{with } S = \begin{pmatrix} \mathbb{1} & 0 \\ 0 & -\mathbb{1} \end{pmatrix}, \tag{2.2}$$

where $D(k)$ has the dimension $n \times n$ and $\mathbb{1}$ is the $n \times n$ identity matrix. For (1+1))d free fermion systems with $U(1)+S$ symmetry, the SPT phases can be detected by the winding

doi:10.6342/NTU202400302

number defined as

$$\begin{aligned} v(D^\dagger) &= \frac{1}{2\pi i}\int_{BZ} dk\ \mathrm{Tr}[(D^\dagger)^{-1}\partial_k D^\dagger], \\ &= \frac{1}{2\pi i}\int_{BZ} dk\ \partial_k \log(\det[D^\dagger]), \end{aligned} \tag{2.3}$$

where BZ denotes the first Brillouin zone, the notation Tr is trace, and det represents the determinant.

Beyond detecting the SPT phases, for systems with open boundary conditions (OBCs), the winding number can be utilized to characterize the number of robust zero-energy edge states as well (see [25] and references therein). This one-to-one relation is bulk-boundary correspondence in (1+1)d free fermion systems with $U(1) + S$ symmetry. For semi-infinite systems, such correspondence can be strictly proven and clearly illustrated using only Cauchy's integral and elementary algebra [44, 45]. Specifically, if we impose OBCs on a semi-infinite system by truncating it without breaking the unit cells, we have

> For right semi-infinite chains, if $v \geq 0$, there are v robust left zero-energy edge states located on $|a, j\rangle$, and if $v \leq 0$, there are $|v|$ robust left zero-energy edge states located on $|b, j\rangle$. (2.4)

and

> For left semi-infinite chains, if $v \geq 0$, there are v robust right zero-energy edge states located on $|b, j\rangle$, and if $v \leq 0$, there are $|v|$ robust right zero-energy edge states located on $|a, j\rangle$. (2.5)

Here, j is the cell index. $|a\rangle$ and $|b\rangle$ denote the basis states of the chiral operator S shown in eq. (2.2) with eigenvalue $+1$ and with eigenvalue -1 respectively, and $|a/b, j\rangle = |a/b\rangle \otimes |j\rangle$.

doi:10.6342/NTU202400302

2.2 Bulk-boundary correspondence in (1+1)d fermionic systems with $U(1)$ and chiral symmetry

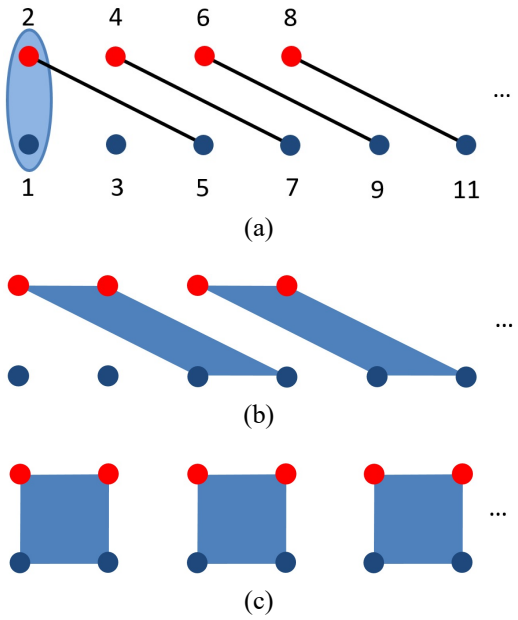

Figure 2.1: (a) The schematic diagram of H_2 where the shadow part represents the unit cell. (b) The schematic diagram of H_{int_2}. (b) The schematic diagram of H_{int_0}.

With the introduction of interaction, the classification of (1+1)d fermionic systems protected by $U(1)+S$ symmetry is reduced from $\mathbb{Z}$ to $\mathbb{Z}_4$, with the SPT phases detectable by the chiral-respecting topological invariant Z^S. Our manner to physically understand the fermionic SPT phases is inspired by the literature [42, 43]. For the chiral symmetry with $Sc_jS^{-1}=(-1)^j c_j^\dagger$, after relabeling fermions as

$$\begin{aligned} c_{2j-1} &= a_j, \qquad & Sa_jS^{-1} &= -a_j^\dagger, \\ c_{2j} &= b_j, \qquad & Sb_jS^{-1} &= b_j^\dagger, \end{aligned} \tag{2.6}$$

we generalize the bulk-boundary correspondence in free fermion (2.4) to fermionic scope and then propose the following relation

$$2\,\mathrm{Arg}[Z^S(H_d)]/\pi = N_b - N_a \bmod 4, \tag{2.7}$$

doi:10.6342/NTU202400302

where H_d denotes the decomposable systems as stated at the beginning of this chapter. $Z^S(H_d)$ represents the corresponding topological invariant Z^S for a given H_d, and N_a (N_b) is the number of unbinding a_j (b_j) of H_d. It's worth noting that this relation is only valid for the chiral symmetry with $Sc_jS^{-1} = (-1)^j c_j^\dagger$ because the value of Z^S depends on the unitary part of chiral symmetry $U_S^{I_1}$. However, since such generalization isn't confined to a certain chiral symmetry, we believe that one can still point out a relation between $Z^S(H_d)$ and $N_b - N_a$ for other chiral symmetry.

2.3 Some examples

	H_2	H_{int_2}	H_{int_0}
$N_b - N_a$	-2	-2	0
Z^S	$-1/64$	$-1/8$	1

Table 2.1: The quantum number $N_b - N_a$ and Z^S for H_2, H_{int_2}, and H_{int_0}. This table shows the relation (2.7) works.

We now examine eq. (2.7) by studying the following lattice models with half-filling as shown in Fig 2.1

$$\begin{aligned} H_2 &= \sum_{j=1} [c_{2j}^\dagger c_{2j+3} + h.c.], \\ H_{int_0} &= \sum_{j=1} [c_{4j-3}^\dagger c_{4j-2}^\dagger c_{4j-1} c_{4j} + h.c.], \\ H_{int_2} &= \sum_{j=1} [c_{4j-2}^\dagger c_{4j}^\dagger c_{4j+1} c_{4j+3} + h.c.]. \end{aligned} \tag{2.8}$$

All three models are decomposable and respect $U(1)$ symmetry (charge conservation) and chiral symmetry $Sc_jS^{-1} = (-1)^j c_j^\dagger$. If we regard H_2 as a free lattice model and describe it in the single-particle basis set, we can evaluate the winding number of H_2, corresponding to the subscript of H_2. H_{int_2} can be viewed as the quartic interaction that couples two

doi:10.6342/NTU202400302

adjacent hopping terms of H_2. For these three models, the quantum number $N_b - N_a$ can be easily determined by seeing Fig 2.1. After evaluating Z^S as shown in Table. 2.1, we see the relation (2.7) established.

Although $N_b - N_a$ can only be assigned to decomposable systems, the relation we established still can play a role when we discuss a system that is not decomposable. If a lattice system can be written as a linear superposition of decomposable systems, we can assign $N_b - N_a$ to its decomposable systems and thus know if it is possible that by tuning parameters, the system has a phase transition. As a concrete example, we construct the following continuous path of Hamiltonians interpolating between two decomposable systems

$$(1-t)H_a + tH_b \quad , t \in [0,1]\,. \tag{2.9}$$

Tuning the parameter t from 0 to 1 in the above equation represents the adiabatic deformation from H_a to H_b, and we simply denote this adiabatic deformation as $H_a \to H_b$ in the latter discussion. Let's focus on the deformation $H_2 \to H_{int_0}$ first. During this deformation, the system can always be considered as a linear superposition of two decomposable systems. By use of eq. (2.7), we know this deforming process will go through two distinct SPT phases, so it should involve a phase transition. Also, according to the same idea, we expect that a phase transition will happen during the deformation $H_{int_2} \to H_{int_0}$ as well. The numerical results in Fig 2.2 agree with these expectations.

As stated in Sec.1.1, within the band theory, topological phase transition determines where the energy gap closes, which is one of the most notable signatures of topological materials. But this trait can be manifested in the thermodynamic limit only, and when

doi:10.6342/NTU202400302

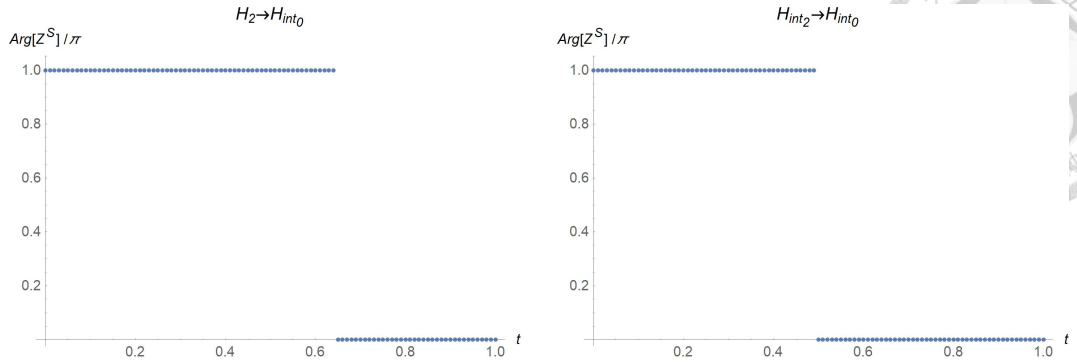

(a) (b)

Figure 2.2: As mentioned in Sec.1.3.1, we evaluate Z^S with the cut and glue construction. (a) The complex phase of Z^S of the deformation $H_2 \to H_{int_0}$. (b) The complex phase of Z^S of the deformation $H_{int_2} \to H_{int_0}$.

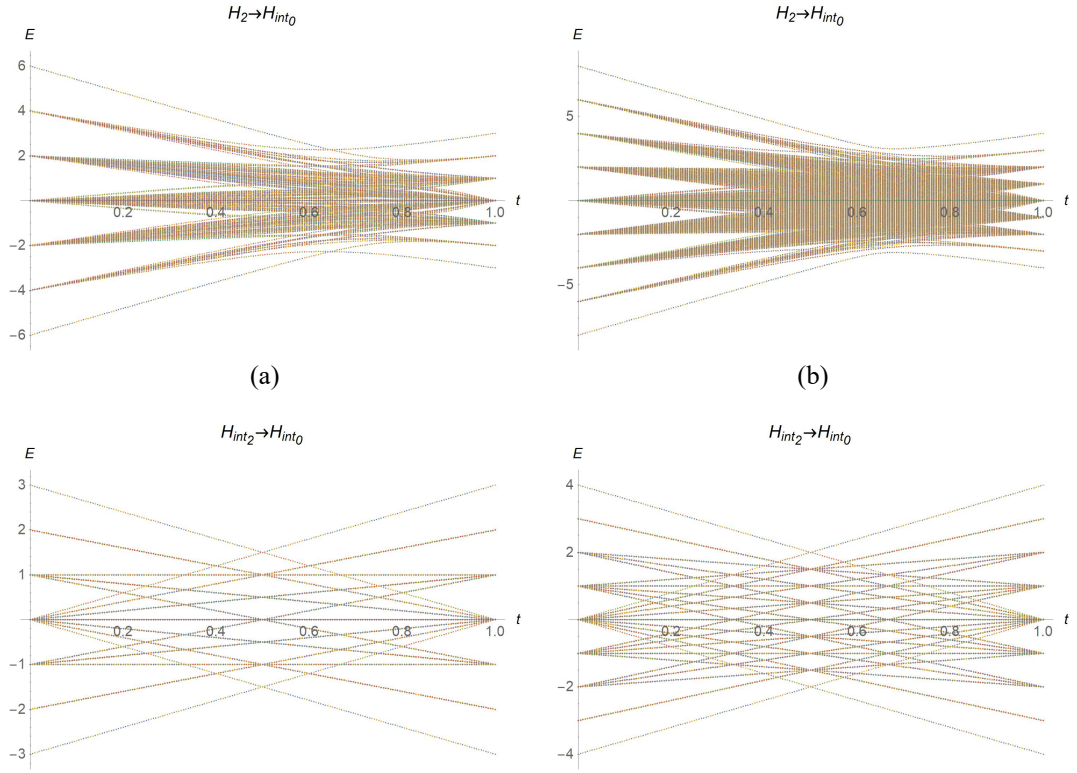

(a) (b)

(c) (d)

Figure 2.3: The eigenvalues of two different systems with PBCs. (a) $H_2 \to H_{int_0}$ with $N_{\text{tot}} = 12$. (b) $H_2 \to H_{int_0}$ with $N_{\text{tot}} = 16$. (c) $H_{int_2} \to H_{int_0}$ with $N_{\text{tot}} = 12$. (d) $H_{int_2} \to H_{int_0}$ with $N_{\text{tot}} = 16$.

it comes to many-body systems, there is no Bloch Hamiltonian that can help us study the behavior of systems in the thermodynamic limit. If we consider the finite-system energy spectrum, this property will be suppressed by the finite-size effect. For free fermion

doi:10.6342/NTU202400302

systems, we can see an energy gap induced by the finite-size effect, but this gap vanishes when the system is in the thermodynamic limit. However, we find that the finite-size effect on many-body systems here is not the same as how it affects free fermion systems. More specifically, for many-body systems with PBCs, we discover that the energy gap may vanish and correspond to the phase transition point even if they suffer from the finite-size effect. As a case in point, we numerically calculate the eigenvalues of $H_2 \to H_{int_0}$ and $H_{int_2} \to H_{int_0}$ as shown in Fig 2.3, which shows the gap-closing happens for both cases when the total number of sites N_{tot} is 12, while when $N_{\text{tot}} = 16$, the gap vanishes only for $H_{int_2} \to H_{int_0}$. Compared with the phase transitions in Fig 2.2, we can see the consistency between the phase transition points and the gap-closing points if the gap-closing occurs. In general, the appearance of this consistency in finite systems is contrary to common belief. Our explanation for this is that it's a kind of unique property of fermionic systems just like the odd-even staggering effect.

doi:10.6342/NTU202400302

Chapter 3

(1+1)d Fermionic SPT Phases Protected by $U(1)$ and Reflection Symmetry

The reflection symmetry R acts on complex fermions as $Rc_jR^{-1} = c_{N_{\text{tot}}-j+1}$ where N_{tot} is the total number of sites. If a lattice Hamiltonian H satisfies $RHR^{-1} = H$, it respects reflection symmetry. The classification of (1+1)d free fermion and fermionic SPT phases protected by $U(1) + R$ symmetry is $\mathbb{Z}$ and $\mathbb{Z}_4$ respectively, which is the same as the cases with $U(1) + S$ symmetry. In fact, the same classifications for these two different kinds of SPT phases can be regarded as a consequence of the CPT (charge-parity-time) theorem. Although the existence of the CPT theorem is under consideration with relativistic symmetry, as stated in Sec.1.2, relativistic symmetry seems to play no role when classifying SPT phases [1].

For the systems with $U(1) + R$ symmetry, there is no bulk-edge correspondence in real space [46], so the idea we used when discussing chiral cases is not applicable to physically understanding the SPT phases here. However, owing to the Atiyah-Hirzebruch spectral sequence (AHSS) in generalized homology, we still can establish a relation between Z^R and decomposable systems. A generalized homology can provide the classification of the SPT phases regarding crystalline symmetry, and AHSS is a way commonly used to compute generalized homology. With the help of AHSS, we will show that the topolog-

[1] Especially, the cobordism classification of (1+1)d fermionic SPT protected by $U(1) + S$ symmetry and protected by $U(1) + R$ symmetry is given by the same cobordism group $\Omega_2^{\text{pin}^c}(pt) = \mathbb{Z}_4$.

doi:10.6342/NTU202400302

ical invariant Z^R actually responds to the quantum number (N_c, R_c) decomposed by an equivalence relation. Here, N_c is the number of charges on the reflection center and is a $\mathbb{Z}$ number. R_c is a $\mathbb{Z}_2$ number and is defined as

$$R_c = \begin{cases} 0, & \text{if } R\psi_c R^{-1} = \psi_c \\ 1, & \text{if } R\psi_c R^{-1} = -\psi_c \end{cases}, \tag{3.1}$$

where ψ_c represents the charges on the reflection center. It's worth noting that since (N_c, R_c) is related to ψ_c, it's a quantum number regarding the reflection center, which is a (0+1)d system. In a manner, the relation between Z^R and (N_c, R_c) we will propose can be read as bulk-boundary correspondence because if we regard the reflection center as the "boundary", this relation implies the information of "boundary" is characterized by the topological invariant Z^R.

3.1 Bulk-boundary correspondence in (1+1)d fermionic systems with $U(1)$ and reflection symmetry

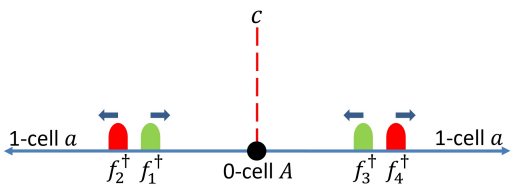

Figure 3.1: The schematic of the first differential $d^1_{1,0}$. The red dashed line denotes the reflection center. The green and red wave packets represent the complex fermions with a charge $+e$ and $-e$, respectively.

To see the relation between Z^R and (N_c, R_c), we should go into detail about generalized homology, which can formulate the SPT phases with crystalline symmetry [17]. In Appendix A, we provide a brief review of how to compute generalized homology by using AHSS. For our cases, the (1+1)d systems with $U(1) + R$ symmetry where the total sym-

doi:10.6342/NTU202400302

metry G is $\mathbb{Z}_2$, the classification is given by $h_0^{\mathbb{Z}_2}(\mathbb{R}, \partial\mathbb{R})$, which describes the SPT phases over $\mathbb{R}$ where anomalies may localize on $\partial\mathbb{R}$. After doing cell decomposition, there are one 0-cell $\{A\}$ respects $U(1) + R$ symmetry and one 1-cell $\{a\}$ with $U(1)$ symmetry, leading to the following E^1-page

$q = 0$	$\mathbb{Z} \times \mathbb{Z}_2$	$\mathbb{Z}$
$q = 1$	0	0
$E^1_{p,-q}$	$p = 0$	$p = 1$

(3.2)

The limiting page here is E^2-page, and hence the classification $h_0^{\mathbb{Z}_2}(\mathbb{R}, \partial\mathbb{R})$ fits into the short exact sequence

$$0 \to E^2_{0,0} \to h_0^{\mathbb{Z}_2}(\mathbb{R}, \partial\mathbb{R}) \to E^2_{1,-1} \to 0. \tag{3.3}$$

By using eq. (A.9), we have

$$\begin{aligned} E^2_{0,0} &= E^1_{0,0}/\mathrm{Im}(d^1_{1,0}), \\ E^2_{1,-1} &= 0. \end{aligned} \tag{3.4}$$

Since $E^2_{1,-1} = 0$, the classification here is given by $h_0^{\mathbb{Z}_2}(\mathbb{R}, \partial\mathbb{R}) \cong E^2_{0,0} = E^1_{0,0}/\mathrm{Im}(d^1_{1,0})$. Without loss of generality, we can assign the quantum number (N_c, R_c) to $E^1_{0,0}$, which is the degree 0 SPT phases on the reflection center, due to the classification $\mathbb{Z} \times \mathbb{Z}_2$. N_c is the number of charges located at the reflection center and R_c is given by eq. (3.1). With the quantum number (N_c, R_c), the quotient $E^1_{0,0}/\mathrm{Im}(d^1_{1,0})$, which essentially represents a process where the SPT states on 0-cell are trivialized by pair-creation of SPT states on adjacent 1-cell [16], can be readily understood. Let's focus on $\mathrm{Im}(d^1_{1,0})$ first. As shown in

doi:10.6342/NTU202400302

Fig 3.1, $d^1_{1,0}$ represents the adiabatic pump as follows: First, we create a pair of complex fermions with a charge $+e$ and $-e$ at the 1-cell $\{a\}$, which is denoted by $f_1^\dagger f_2^\dagger$, then, we move them and their reflection counterparts $f_3^\dagger f_4^\dagger$ to the reflection center and the infinity while preserving reflection symmetry. This adiabatic pump makes $f_1^\dagger f_3^\dagger$ located at the reflection center (0-cell $\{A\}$), so we can assign (N_c, R_c) to $f_1^\dagger f_3^\dagger$, which is given by $(2,1)$ because $Rf_1^\dagger f_3^\dagger R^{-1} = f_3^\dagger f_1^\dagger = -f_1^\dagger f_3^\dagger$. Given that this procedure can be repeated many times, we have $\mathrm{Im}(d^1_{1,0}) = \mathbb{Z}(2,1)$, which leads to $E^1_{0,0}/\mathrm{Im}(d^1_{1,0}) \cong \mathbb{Z}\times\mathbb{Z}_2/\mathbb{Z}(2,1) \cong \mathbb{Z}_4$. More specifically, the equivalence relation of the quotient $E^1_{0,0}/\mathrm{Im}(d^1_{1,0})$ can be written as

$$(N_c, R_c) + n(2,1) \sim (N_c, R_c), \quad n \in \mathbb{Z}, \tag{3.5}$$

and the corresponding equivalence classes can be defined as $[(0,0)], [(1,0)], [(2,0)]$, and $[(3,0)]$. Since the generalized homology $h_0^{\mathbb{Z}_2}(\mathbb{R}, \partial\mathbb{R})$ is isomorphic to $E^1_{0,0}/\mathrm{Im}(d^1_{1,0})$, the classification of (1+1)d systems with $U(1) + R$ symmetry is $\mathbb{Z}_4$, and we can assign the quantum number (N_c, R_c) decomposed by the equivalence relation (3.5) to decomposable systems. As stated above, the classification also can be provided by the cobordism group $\Omega_2^{\mathrm{pin}^c}(pt) = \mathbb{Z}_4$, which is consistent with $h_0^{\mathbb{Z}_2}(\mathbb{R}, \partial\mathbb{R})$. This consistency implies that we may connect Z^R, which is the topological invariant generated by the cobordism group, and (N_c, R_c) in a certain way. Here we suggest that

$$(N_c, R_c) \sim (2\,\mathrm{Arg}[Z^R(H_d)]/\pi, 0), \quad \text{for } \alpha = -\pi/2. \tag{3.6}$$

For a given decomposable system H_d, we can assign the quantum number (N_c, R_c) to it and evaluate its corresponding topological invariant $Z^R(H_d)$. In the rest of this discussion, we will show that eq. (3.6) makes sense by studying some examples.

doi:10.6342/NTU202400302

3.2 Example: SSH models

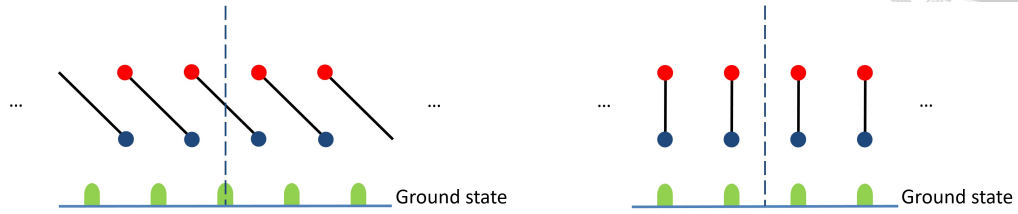

(a) (b)

Figure 3.2: The dashed line is the reflection center and the green wave packets represent the charges. (a) By decomposing the ground states, we obtain $\psi_c(H_1) = (c^\dagger_{L+1} - c^\dagger_{L+2})/\sqrt{2}$ and $\psi_c(-H_1) = (c^\dagger_{L+1} + c^\dagger_{L+2})/\sqrt{2}$. Hence, the number of charges located at the reflection center is $N_c = 1$ for H_1 and $-H_1$ both. (b) For $\pm H_0$, there is no charge located at the reflection center, so $\psi_c(H_0) = \psi_c(-H_0) = 0$.

Here we verify eq. (3.6) by studying the SSH model with half-filling in the topological and trivial limits

$$\begin{aligned} H_1 &= \sum_{j=1}^{L} [c^\dagger_{2j} c_{2j+1} + c^\dagger_{2L+2} c_1 + h.c.], \\ H_0 &= \sum_{j=1}^{L+1} [c^\dagger_{2j-1} c_{2j} + h.c.]. \end{aligned} \tag{3.7}$$

To evaluate the topological invariant Z^R, the boundary condition here is PBC. Their ground states are given by

$$\begin{aligned} |GS(H_1)\rangle = \frac{1}{2^{(L+1)/2}} &(c^\dagger_2 - c^\dagger_3)(c^\dagger_4 - c^\dagger_5) \dots (c^\dagger_{2N} - c^\dagger_{2N+1}) \dots (c^\dagger_{2M} - c^\dagger_{2M+1}) \dots \\ &(c^\dagger_{2L+2} - c^\dagger_1) |0\rangle , \\ |GS(H_0)\rangle = \frac{1}{2^{(L+1)/2}} &(c^\dagger_1 - c^\dagger_2)(c^\dagger_3 - c^\dagger_4) \dots (c^\dagger_{2N+1} - c^\dagger_{2N+2}) \dots (c^\dagger_{2M-1} - c^\dagger_{2M}) \dots \\ &(c^\dagger_{2L+1} - c^\dagger_{2L+2}) |0\rangle . \end{aligned} \tag{3.8}$$

The finite systems H_1 and H_0 contain $L+1$ unit cells, and there are two sites in each unit cell. If we also consider the chiral symmetry, their subscripts denote the corresponding winding numbers. Note that they respect reflection symmetry $Rc^\dagger_j R^{-1} = c^\dagger_{2L+3-j}$, and

doi:10.6342/NTU202400302

hence we can pick up the interval $I = \{c_a, \ldots, c_b\}$ where its center is the same as reflection center to define the partial reflection $[U_\alpha R]_I$ as

$$[U_\alpha R]_I c_j^\dagger ([U_\alpha R]_I)^{-1} = i c_{2L+3-j}^\dagger \quad [U_\alpha R]_I |0\rangle = |0\rangle , \quad j \in \{a, \ldots, b\}. \tag{3.9}$$

Here we suppose $a < b$ and $a + b = 2L + 3$. By definition, we can evaluate the corresponding Z^R (Appendix B), which is given by

$$\begin{aligned} Z^R(H_1) &= \frac{i^{(N_\mathrm{p}-1)}}{2}(-1)^{(N_\mathrm{p}-1)(N_\mathrm{p}-2)/2}(-1)^{(N_\mathrm{p}-1)} = (-1)^{N_\mathrm{p}-1}\frac{i^{(N_\mathrm{p}-1)^2}}{2}, \\ Z^R(H_0) &= (-1)^{N_\mathrm{p}}(-1)^{N_\mathrm{p}(N_\mathrm{p}-1)/2} i^{N_\mathrm{p}} = (-1)^{N_\mathrm{p}} i^{N_\mathrm{p}^2}, \end{aligned} \tag{3.10}$$

where $N_\mathrm{p} = (b - a + 1)/2$. Now, let's focus on the same systems with negative hopping strength. The explicit expressions of the ground states of $-H_1$ and $-H_0$ can be written as

$$\begin{aligned} |GS(-H_1)\rangle = \frac{1}{2^{(L+1)/2}}&(c_2^\dagger + c_3^\dagger)(c_4^\dagger + c_5^\dagger)\ldots(c_{2N}^\dagger + c_{2N+1}^\dagger)\ldots(c_{2M}^\dagger + c_{2M+1}^\dagger)\ldots \\ &(c_{2L+2}^\dagger + c_1^\dagger)|0\rangle , \\ |GS(-H_0)\rangle = \frac{1}{2^{(L+1)/2}}&(c_1^\dagger + c_2^\dagger)(c_3^\dagger + c_4^\dagger)\ldots(c_{2N+1}^\dagger + c_{2N+2}^\dagger)\ldots(c_{2M-1}^\dagger + c_{2M}^\dagger)\ldots \\ &(c_{2L+1}^\dagger + c_{2L+2}^\dagger)|0\rangle . \end{aligned} \tag{3.11}$$

By the same token, we obtain

$$\begin{aligned} Z^R(-H_1) &= (-1)^{-(N_\mathrm{p}-1)} Z^R(H_1), \\ Z^R(-H_0) &= (-1)^{-N_\mathrm{p}} Z^R(H_0). \end{aligned} \tag{3.12}$$

If the reflection center is located between two unit cells (bond center), that is, N_p is even, the above equation leads to $Z^R(-H_1) = -Z^R(H_1)$ and $Z^R(-H_0) = Z^R(H_0)$. One may wonder why $\pm H_0$ are in the same SPT phase, but $\pm H_1$ fall into different SPT phases. To figure out this point, let's assign the quantum number (N_c, R_c) to these four cases. For the

doi:10.6342/NTU202400302

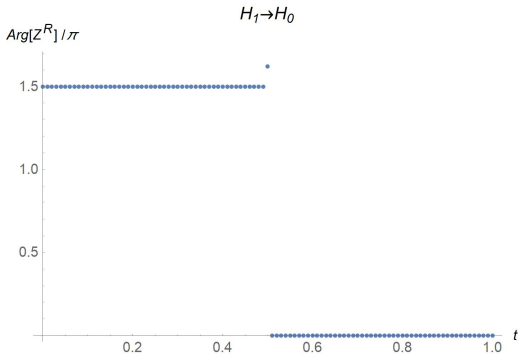

Figure 3.3: The complex phase of Z^R of the deformation $H_1 \to H_0$ with the bond center. The total number of sites is $N_{\text{tot}} = 12$, and the interval we pick up is $I = \{c_4, \ldots, c_9\}$.

	H_1	$-H_1$	H_0	$-H_0$
(N_c, R_c)	$(1,1)$	$(1,0)$	$(0,0)$	$(0,0)$
Z^R	$-i/2$	$i/2$	1	1

Table 3.1: The quantum number (N_c, R_c) and Z^R for $\pm H_0$ and $\pm H_1$ with the bond center. Note that $(1,1) \sim (3,0)$.

decomposable systems, such as eq. (2.8) and eq. (3.7), their ground states can be written as the tensor product of separated charges, so the information of ψ_c can be easily obtained by seeing their ground states. As Fig 3.2, ψ_c of the cases we study now are given by

$$\begin{aligned}
&\psi_c(H_1) = \frac{c^\dagger_{L+1} - c^\dagger_{L+2}}{\sqrt{2}}, && R\psi_c(H_1)R^{-1} = -\psi_c(H_1),\\
&\psi_c(-H_1) = \frac{c^\dagger_{L+1} + c^\dagger_{L+2}}{\sqrt{2}}, && R\psi_c(-H_1)R^{-1} = \psi_c(H_1),\\
&\psi_c(H_0) = 0, && R\psi_c(H_0)R^{-1} = \psi_c(H_0),\\
&\psi_c(-H_0) = 0, && R\psi_c(-H_0)R^{-1} = \psi_c(H_0).
\end{aligned} \tag{3.13}$$

With eq. (3.1) and eq. (3.13), the corresponding (N_c, R_c) can be determined as shown in Table 3.1. Obviously, for the bond center, there are no charges on the reflection center for $\pm H_0$, so they are both trivial, which is consistent with $Z^R(-H_0) = Z^R(H_0)$. For $\pm H_1$, although $N_c = 1$ for both cases, they have different R_c, so they belong to different SPT phases, which corresponds to $Z^R(-H_1) = -Z^R(H_1)$. Taking all these into account and

doi:10.6342/NTU202400302

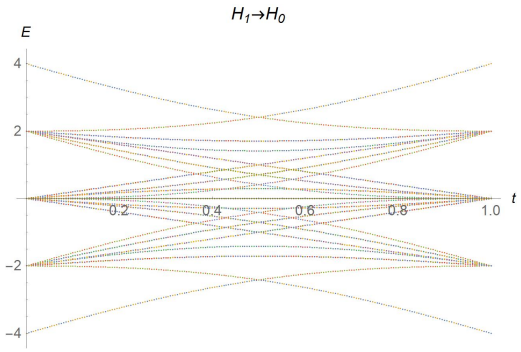

(a)

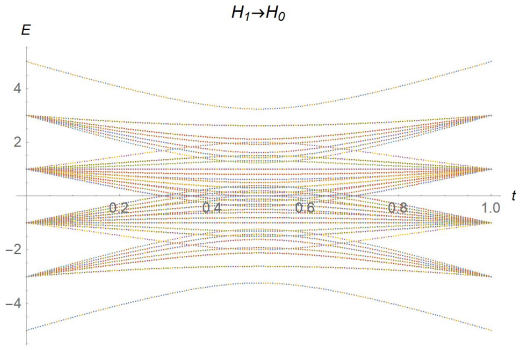

(b)

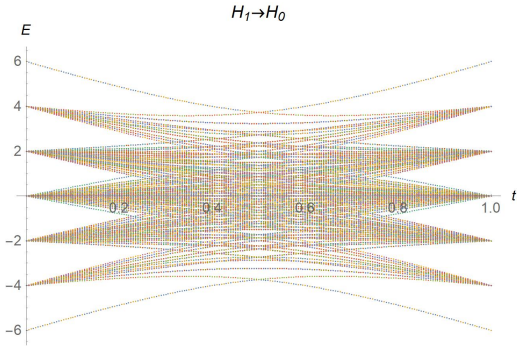

(c)

Figure 3.4: The eigenvalues of $H_1 \to H_0$ with PBC. Because of PBCs, the systems here respect two different types of reflection symmetry where the reflection center is located at the midpoint of a unit cell or between two unit cells. Therefore, The information regarding these two different types of reflection symmetry is contained in their eigenvalue spectra simultaneously. (a) $N_{\text{tot}} = 8$. (b) $N_{\text{tot}} = 10$. (c) $N_{\text{tot}} = 12$.

comparing with Z^R as shown in Table 3.1, we can see the relation (3.6) is valid. On the other hand, the same argument regarding the finite-system energy spectrum we made when discussing chiral cases also holds here. As shown in Fig 3.3, a phase transition happens at the midpoint of the deformation $H_1 \to H_0$. Compared with Fig 3.4, when the total number of sites N_{tot} is 8 or 12, we can see that the gap-closing points of finite systems

doi:10.6342/NTU202400302

with PBCs are the same as the phase transition point.

3.3 Example: systems with quartic interaction

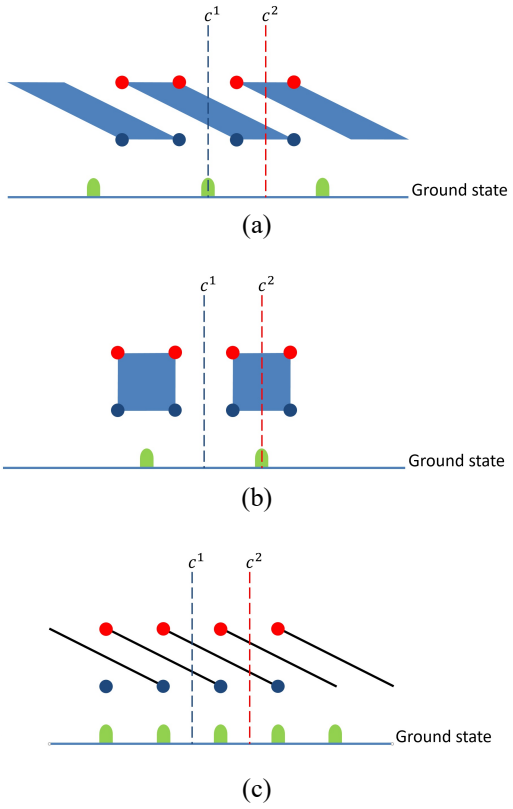

Figure 3.5: Different reflection centers make the topology different. (a) When the reflection center is c^1, the quantum numbers (N_c, R_c) of H_{int_2} and $-H_{int_2}$ are $(2,1)$ and $(2,0)$. For the cases with c^2, there is no charge located at the bond center, and hence $\pm H_{int_2}$ are topologically trivial. (b) $\pm H_{int_0}$ are topologically trivial for c^1. If the reflection center is c^2, we can assign $(2,1)$ and $(2,0)$ to H_{int_0} and $-H_{int_0}$. (c) $\pm H_2$ are topologically trivial for both reflection centers.

When discussing the SSH models with $U(1) + R$ symmetry, we saw that the topological invariant Z^R of these (1+1)d systems depends on where the reflection center is, which is expected since the SPT phases here are actually related to the SPT phases on the reflection center (0-cell $\{A\}$). To emphasize this fact, we now study the systems we introduced before, H_2, H_{int_2}, and H_{int_0}. They also respect reflection symmetry with $Rc_jR^{-1} = c_{N_{\text{tot}}-j+1}$. Let's focus on the systems with quartic interaction first. The ground

doi:10.6342/NTU202400302

	H_{int_2}	$-H_{int_2}$	H_{int_0}	$-H_{int_0}$	H_2	$-H_2$
(N_{c^1}, R_{c^1})	$(2,1)$	$(2,0)$	$(0,0)$	$(0,0)$	$(0,0)$	$(0,0)$
$Z^R_{c^1}$	$1/2$	$-1/2$	1	1	$1/4$	$1/4$
(N_{c^2}, R_{c^2})	$(0,0)$	$(0,0)$	$(2,1)$	$(2,0)$	$(0,0)$	$(0,0)$
$Z^R_{c^2}$	$1/2$	$1/2$	1	-1	$1/4$	$1/4$

Table 3.2: The quantum number (N_c, R_c) and the topological invariant Z^R for the different systems, $\pm H_{int_2}$, $\pm H_{int_0}$, and $\pm H_2$, with the reflection centers c^1 and c^2.

states of $\pm H_{int_2}$ and $\pm H_{int_0}$ with PBCs can be explicitly written as

$$\begin{aligned}|GS(H_{int_2})\rangle = \frac{1}{2^{(L+1)/2}}&(c_2^\dagger c_4^\dagger + c_5^\dagger c_7^\dagger)(c_6^\dagger c_8^\dagger + c_9^\dagger c_{11}^\dagger)\dots(c_{4N-2}^\dagger c_{4N}^\dagger + c_{4N+1}^\dagger c_{4N+3}^\dagger)\dots \\ &(c_{4M-2}^\dagger c_{4M}^\dagger + c_{4M+1}^\dagger c_{4M+3}^\dagger)\dots(c_{4L+2}^\dagger c_{4L+4}^\dagger + c_1^\dagger c_3^\dagger)\,|0\rangle\,, \\ |GS(-H_{int_2})\rangle = \frac{1}{2^{(L+1)/2}}&(c_2^\dagger c_4^\dagger - c_5^\dagger c_7^\dagger)(c_6^\dagger c_8^\dagger - c_9^\dagger c_{11}^\dagger)\dots(c_{4N-2}^\dagger c_{4N}^\dagger - c_{4N+1}^\dagger c_{4N+3}^\dagger)\dots \\ &(c_{4M-2}^\dagger c_{4M}^\dagger - c_{4M+1}^\dagger c_{4M+3}^\dagger)\dots(c_{4L+2}^\dagger c_{4L+4}^\dagger - c_1^\dagger c_3^\dagger)\,|0\rangle\,,\end{aligned} \tag{3.14}$$

and

$$\begin{aligned}|GS(H_{int_0})\rangle = \frac{1}{2^{(L+1)/2}}&(c_1^\dagger c_2^\dagger + c_3^\dagger c_4^\dagger)(c_5^\dagger c_6^\dagger + c_7^\dagger c_8^\dagger)\dots(c_{4N+1}^\dagger c_{4N+2}^\dagger + c_{4N+3}^\dagger c_{4N+4}^\dagger)\dots \\ &(c_{4M-3}^\dagger c_{4M-2}^\dagger + c_{4M-1}^\dagger c_{4M}^\dagger)\dots(c_{4L+1}^\dagger c_{4L+2}^\dagger + c_{4L+3}^\dagger c_{4L+4}^\dagger)\,|0\rangle\,, \\ |GS(-H_{int_0})\rangle = \frac{1}{2^{(L+1)/2}}&(c_1^\dagger c_2^\dagger - c_3^\dagger c_4^\dagger)(c_5^\dagger c_6^\dagger - c_7^\dagger c_8^\dagger)\dots(c_{4N+1}^\dagger c_{4N+2}^\dagger - c_{4N+3}^\dagger c_{4N+4}^\dagger)\dots \\ &(c_{4M-3}^\dagger c_{4M-2}^\dagger - c_{4M-1}^\dagger c_{4M}^\dagger)\dots(c_{4L+1}^\dagger c_{4L+2}^\dagger - c_{4L+3}^\dagger c_{4L+4}^\dagger)\,|0\rangle\,.\end{aligned} \tag{3.15}$$

Here we consider the finite systems with $N_{\text{tot}} = 4L + 4$. As an analogy of unit cells, here we introduce the concept of a "subsystem" that contains four sites, so these finite systems have $L+1$ subsystems. Given that $\pm H_{int_2}$ respect reflection symmetry $Rc_j^\dagger R^{-1} = c_{4L+5-j}^\dagger$, we can choose the interval $I = \{c_a, \dots, c_b\}$ with $a < b$ and $a + b = 4L + 5$ to define the partial reflection

$$[U_\alpha R]_I c_j^\dagger ([U_\alpha R]_I)^{-1} = i c_{4(L+1)-j+1}^\dagger, \quad [U_\alpha R]_I\,|0\rangle = |0\rangle\,, \tag{3.16}$$

doi:10.6342/NTU202400302

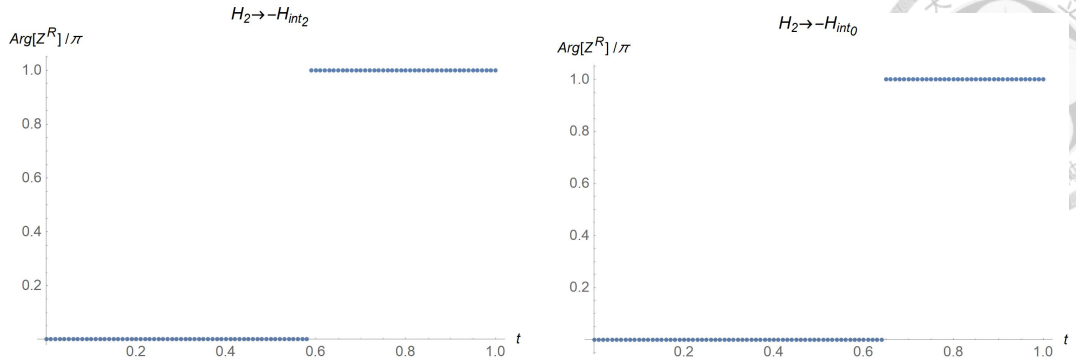

(a) (b)

Figure 3.6: For the reflection center c^1, we consider the finite system with $N_{\text{tot}} = 16$, and then pick up the interval $I = \{c_5, \ldots, c_{12}\}$. The interval $I = \{c_5, \ldots, c_8\}$ in the finite system with $N_{\text{tot}} = 12$ is assigned to the reflection center c^2. (a) The complex phase of Z^R of the deformation $H_2 \to -H_{int_2}$ with c^1. (b) The complex phase of Z^R of the deformation $H_2 \to -H_{int_0}$ with c^2.

with $j \in \{a, \ldots, b\}$. We can employ the same method as discussing $\pm H_1$ and $\pm H_0$ to find the SPT phases $\pm H_{int_2}$ and $\pm H_{int_0}$ fall into. Obviously, there are two different types of reflection centers where one is situated between two subsystems and the other is in the midpoint of a subsystem. we label them c^1 and c^2. As Fig 3.5(a), we have

$$\begin{aligned}
\psi_{c^1}(H_{int_2}) &= \frac{c^\dagger_{2(L+1)-2}c^\dagger_{2(L+1)} + c^\dagger_{2(L+1)+1}c^\dagger_{2(L+1)+3}}{\sqrt{2}}, \\
\psi_{c^1}(-H_{int_2}) &= \frac{c^\dagger_{2(L+1)-2}c^\dagger_{2(L+1)} - c^\dagger_{2(L+1)+1}c^\dagger_{2(L+1)+3}}{\sqrt{2}}, \\
\psi_{c^2}(H_{int_0}) &= \frac{c^\dagger_{2L+1}c^\dagger_{2L+2} + c^\dagger_{2L+3}c^\dagger_{2L+4}}{\sqrt{2}}, \\
\psi_{c^2}(-H_{int_0}) &= \frac{c^\dagger_{2L+1}c^\dagger_{2L+2} - c^\dagger_{2L+3}c^\dagger_{2L+4}}{\sqrt{2}},
\end{aligned} \tag{3.17}$$

with

$$\begin{aligned}
R\psi_{c^1}(H_{int_2})R^{-1} &= -\psi_{c^1}(H_{int_2}), \\
R\psi_{c^1}(-H_{int_2})R^{-1} &= \psi_{c^1}(-H_{int_2}), \\
R\psi_{c^2}(H_{int_0})R^{-1} &= -\psi_{c^2}(H_{int_0}), \\
R\psi_{c^2}(-H_{int_0})R^{-1} &= \psi_{c^2}(-H_{int_0}).
\end{aligned} \tag{3.18}$$

doi:10.6342/NTU202400302

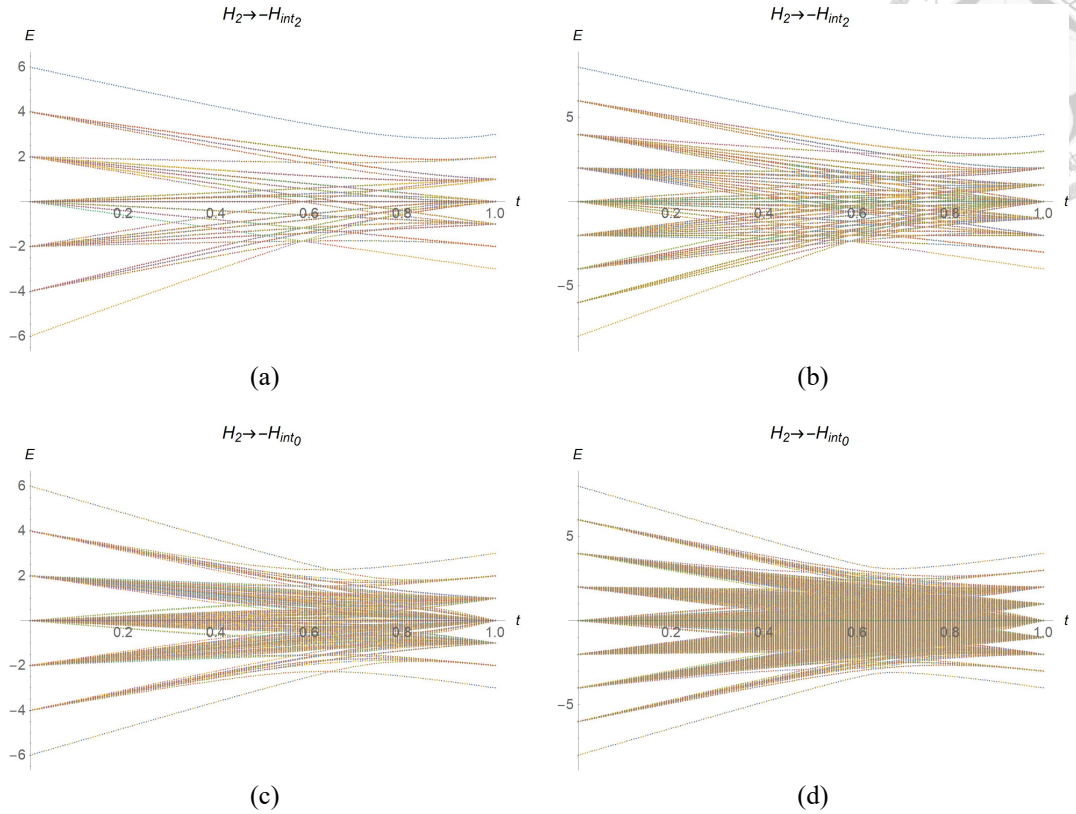

Figure 3.7: The eigenvalues of two different systems with PBCs. These eigenvalue spectra encapsulate the information regarding c^1 and c^2 because the systems with PBCs respect the reflection symmetry with c^1 and c^2 at the same time. (a) $H_2 \to -H_{int_2}$ with $N_{\text{tot}} = 12$. (b) $H_2 \to -H_{int_2}$ with $N_{\text{tot}} = 16$. (c) $H_2 \to -H_{int_0}$ with $N_{\text{tot}} = 12$. (d) $H_2 \to -H_{int_0}$ with $N_{\text{tot}} = 16$.

The corresponding quantum numbers are shown in Table 3.2. Notice that H_{int_0} and H_{int_2} are topologically trivial for both reflection centers because $(2, 1) \sim (0, 0)$. Table 3.2 also shows the SPT phases of $\pm H_2$ with c^1 and c^2, which can be quickly determined by seeing Fig 3.5(b). As a double-check, we can evaluate Z^R for these cases with different reflection centers, where the results are also contained in Table 3.2, and then check the correctness of eq. (3.6). In accordance with Table 3.2, we expect that phase transitions happen for $H_2 \to -H_{int_2}$ with c^1 and $H_2 \to -H_{int_0}$ with c^2. Fig 3.6 agrees with these expectations. In addition, by comparing Fig 3.6 and Fig 3.7, we can see that the argument regarding the gap-closing of finite systems and phase transition we proposed before works.

doi:10.6342/NTU202400302

Chapter 4

Role of Translation Symmetry

In this chapter, we discuss how the fermionic SPT phases we focused on before change when translation symmetry gets involved. First, because the translation symmetry is spatial symmetry and the chiral symmetry is on-site symmetry, there is no interplay between them and hence there is no new SPT phase induced by the combination of $U(1)+S$ and translation symmetry. However, since both translation symmetry and reflection symmetry are spatial symmetry, new SPT phases related to the combination of these two symmetries may emerge. In the latter discussion, we will show that the (1+1)d fermionic SPT phases protected by $U(1)+R$ and translation symmetry are classified by $\mathbb{Z}\times\mathbb{Z}_2\times\mathbb{Z}_4$ (see Sec.4.1).

On the other hand, it's worth noting that translation symmetry is not an element of a point group, so the cobordism group $\Omega_2^{\text{pin}^c}(pt)$ itself does not include translation symmetry, making the classification cannot be given by $\Omega_2^{\text{pin}^c}(pt)$ and the corresponding many-body topological invariant cannot be constructed by the method we mentioned in Sec. 1.3. However, with the help of generalized homology, we indicate that the topological invariants can be constructed in an alternative way, which is given by

$$(Z_f, 2\,\text{Arg}[Z_c^R]/\pi, 2\,\text{Arg}[Z_{c'}^R]/\pi). \tag{4.1}$$

Here we express the translation as the composition of two reflections with reflection cen-

doi:10.6342/NTU202400302

ters c and c'. Thus, Z_c^R and $Z_{c'}^R$ denote the topological invariants (1.5) with respect to c and c', and Z_f is defined as

$$Z_f = \frac{\langle GS| \hat{N} |GS\rangle}{L}, \tag{4.2}$$

where $\hat{N}$ is the particle number operator, L is the number of subsystems, and Z_f is $filling$. We will prove that $(Z_f, 2\,\mathrm{Arg}[Z_c^R]/\pi, 2\,\mathrm{Arg}[Z_{c'}^R]/\pi)$ is sufficient to describe this $\mathbb{Z} \times \mathbb{Z}_2 \times \mathbb{Z}_4$ classification and then apply this set of topological invariants to some examples.

4.1 (1+1)d fermionic systems with $U(1) + R$ and translation symmetry

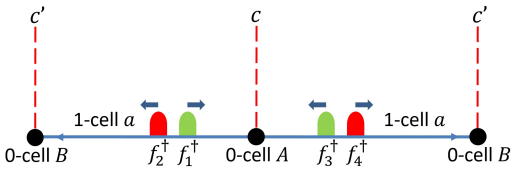

Figure 4.1: The cell decomposition and schematic of the first differential $d^1_{1,0}$ for (1+1)d fermionic systems with $U(1) + R$ and translation symmetry. Note that the adiabatic pump is almost the same as that of the systems without translation symmetry. The only difference is $f_3^\dagger$ and $f_4^\dagger$ will meet on c' instead of going to infinity, so $\mathrm{Im}(d^1_{1,0}) = \mathbb{Z}(2, 1, -2, 1)$ here.

In addition to $U(1) + R$ symmetry, now we involve the translation symmetry $\mathbb{Z} \ni n$: $x \to x + n$. Because the reflection here $r \in \mathbb{Z}_2$ acts on $\mathbb{Z}$ as reflection, the total symmetry G becomes $\mathbb{Z} \rtimes \mathbb{Z}_2$. After doing cell decomposition shown in Fig 4.1, we have two 0-cells $\{A, B\}$, which correspond to the reflection centers $\{c, c'\}$ and respect $U(1) + R$ symmetry, and a 1-cell $\{a\}$ with $U(1)$ symmetry, leading to the following E^1-page

doi:10.6342/NTU202400302

$q=0$	$(\mathbb{Z}\times\mathbb{Z}_2)\times(\mathbb{Z}\times\mathbb{Z}_2)$	$\mathbb{Z}$
$q=1$	0	0
$E^1_{p,-q}$	$p=0$	$p=1$

(4.3)

Given that the limiting page here is E^2-page, the classification $h_0^{\mathbb{Z}\times\mathbb{Z}_2}(\mathbb{R},\partial\mathbb{R})$ fits into the short exact sequence

$$0\to E^2_{0,0}\to h_0^{\mathbb{Z}\times\mathbb{Z}_2}(\mathbb{R},\partial\mathbb{R})\to E^2_{1,-1}\to 0. \tag{4.4}$$

By using eq. (A.9), these E^2-pages are given by

$$\begin{aligned} E^2_{0,0} &= E^1_{0,0}/\mathrm{Im}(d^1_{1,0}),\\ E^2_{1,-1} &= 0, \end{aligned} \tag{4.5}$$

which leads to $h_0^{\mathbb{Z}\times\mathbb{Z}_2}(\mathbb{R},\partial\mathbb{R})\cong E^1_{0,0}/\mathrm{Im}(d^1_{1,0})$. As discussed in Sec. 3.1, we can assign the quantum number $(N_c,R_c,N_{c'},R_{c'})$ to $E^1_{0,0}$ here, and $\mathrm{Im}(d^1_{1,0})$ represents the adiabatic pump shown in Fig 4.1, so we have

$$\begin{aligned} h_0^{\mathbb{Z}\times\mathbb{Z}_2}(\mathbb{R},\partial\mathbb{R}) &\cong E^1_{0,0}/\mathrm{Im}(d^1_{1,0}) \cong (\mathbb{Z}\times\mathbb{Z}_2\times\mathbb{Z}\times\mathbb{Z}_2)/\mathbb{Z}(2,1,-2,1)\\ &\cong \mathbb{Z}\times\mathbb{Z}_2\times\mathbb{Z}_4. \end{aligned} \tag{4.6}$$

When we consider the systems without translation symmetry, we use (N_c,R_c) to describe their SPT phases. For a given system, (N_c,R_c) is not unique because we can move the charges in 1-cell to the reflection center while preserving reflection symmetry. But note that, because of eq. (3.5), it will not change the topology of the system, although (N_c,R_c)

doi:10.6342/NTU202400302

will be different. However, for the cases with translation symmetry, we should impose a restriction to $(N_c, R_c, N_{c'}, R_{c'})$. Due to the common sense about translation symmetry where $\mathbb{Z}$ is related to the number of charges in each subsystem, we have

$$Z_f = N_c + N_{c'}. \tag{4.7}$$

That is, in a subsystem, we have to make all the charges located at two reflection centers only. The reason is that we require $(N_c, R_c, N_{c'}, R_{c'})$ to represent an SPT phase in $\mathbb{Z} \times \mathbb{Z}_2 \times \mathbb{Z}_4$ classification, and if we don't consider the restriction (4.7), $(N_c, R_c, N_{c'}, R_{c'})$ will not give us correct information about $\mathbb{Z}$. There are some examples about this argument when we discuss cases with translation symmetry $j \to j + 4$ (see Sec. 4.3).

The idea of employing eq. (4.1) to describe $\mathbb{Z} \times \mathbb{Z}_2 \times \mathbb{Z}_4$ classification is based on two reasons. First, since the whole system respects $U(1)$ and translation symmetry, it's straightforward to think $\mathbb{Z}$ is related to the number of charges in each subsystem, which corresponds to Z_f. Secondly, recall that for the cases without translation symmetry, Z^R responds to the quantum number (N_c, R_c). We can extend this consistency to the systems with translation symmetry. Because the SPT phases can be determined by the (0+1)d SPT phases on two different reflection centers separately, which is described by $(N_c, R_c, N_{c'}, R_{c'})$, we can naively conceive that Z_c^R and $Z_{c'}^R$ may serve as a part of the topological invariants here. Taking these into account, we speculate $(Z_f, 2\,\mathrm{Arg}[Z_c^R]/\pi, 2\,\mathrm{Arg}[Z_{c'}^R]/\pi)$ can be assigned to this $\mathbb{Z} \times \mathbb{Z}_2 \times \mathbb{Z}_4$ classification. Our strategy to prove this surmise is right is as follows. We first find the generators of $\mathbb{Z}$, $\mathbb{Z}_2$, and $\mathbb{Z}_4$ in terms of quantum numbers $(N_c, R_c, N_{c'}, R_{c'})$, which are denoted as $g_{\mathbb{Z}}$, $g_{\mathbb{Z}_2}$, and

doi:10.6342/NTU202400302

$g_{\mathbb{Z}_4}$. Then we consider the following statements

$$\begin{aligned}
&(Z_f(H(g_{\mathbb{Z}})), 2\,\mathrm{Arg}[Z_c^R(H(g_{\mathbb{Z}}))]/\pi, 2\,\mathrm{Arg}[Z_{c'}^R(H(g_{\mathbb{Z}}))]/\pi) \in \mathbb{Z},\\
&(Z_f(H(g_{\mathbb{Z}_2})), 2\,\mathrm{Arg}[Z_c^R(H(g_{\mathbb{Z}_2}))]/\pi, 2\,\mathrm{Arg}[Z_{c'}^R(H(g_{\mathbb{Z}_2}))]/\pi) \in \mathbb{Z}_2,\\
&(Z_f(H(g_{\mathbb{Z}_4})), 2\,\mathrm{Arg}[Z_c^R(H(g_{\mathbb{Z}_4}))]/\pi, 2\,\mathrm{Arg}[Z_{c'}^R(H(g_{\mathbb{Z}_4}))]/\pi) \in \mathbb{Z}_4,
\end{aligned} \tag{4.8}$$

where $H(g_x)$ is the corresponding decomposable system of g_x. If the above statements are satisfied, this classification can be described by the set of topological invariants (4.1). As the first step, we choose the following set of generators

$$\begin{aligned}
g_{\mathbb{Z}} &= (1,0,0,0),\\
g_{\mathbb{Z}_2} &= (0,1,0,0),\\
g_{\mathbb{Z}_4} &= (1,0,-1,0).
\end{aligned} \tag{4.9}$$

As shown in Appendix C, for these three generators, we have

$$\begin{aligned}
&(Z_f(H(ng_{\mathbb{Z}})), 2\,\mathrm{Arg}[Z_c^R(H(ng_{\mathbb{Z}}))]/\pi, 2\,\mathrm{Arg}[Z_{c'}^R(H(ng_{\mathbb{Z}}))]/\pi) = (n, n \bmod 4, 0) \in \mathbb{Z},\\
&(Z_f(H(ng_{\mathbb{Z}_2})), 2\,\mathrm{Arg}[Z_c^R(H(ng_{\mathbb{Z}_2}))]/\pi, 2\,\mathrm{Arg}[Z_{c'}^R(H(ng_{\mathbb{Z}_2}))]/\pi) = (0, 2n \bmod 4, 0) \in \mathbb{Z}_2,\\
&(Z_f(H(ng_{\mathbb{Z}_4})), 2\,\mathrm{Arg}[Z_c^R(H(ng_{\mathbb{Z}_4}))]/\pi, 2\,\mathrm{Arg}[Z_{c'}^R(H(ng_{\mathbb{Z}_4}))]/\pi) = (0, n \bmod 4, 3n \bmod 4) \in \mathbb{Z}_4,
\end{aligned} \tag{4.10}$$

where n is an integer, and $H(ng) = \bigoplus_{i=1}^{n} H(g)$. The above equation satisfies the statements in eq. (4.8), so $(Z_f, 2\,\mathrm{Arg}[Z_c^R]/\pi, 2\,\mathrm{Arg}[Z_{c'}^R]/\pi)$ can be used to describe $\mathbb{Z}\times\mathbb{Z}_2\times\mathbb{Z}_4$ classification.

4.2 Example: translation symmetry $j \to j+2$

If systems respect $U(1)+R$ symmetry and the translation symmetry: $j \to j+2$, it implies that they respect two kinds of reflection symmetries where the reflection cen-

doi:10.6342/NTU202400302

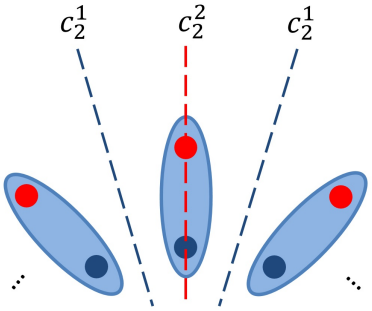

Figure 4.2: Two types of reflection centers for the systems that respect $U(1)+R$ and the translation symmetry: $j \to j+2$.

ters are shown in Fig 4.2. In our systems, H_0, H_1, and H_2 respect this kind of symmetry, and we can get corresponding $(Z_f, 2\,\mathrm{Arg}[Z^R_{c_2^1}]/\pi,\, 2\,\mathrm{Arg}[Z^R_{c_2^2}]/\pi)$ by studying their $(N_{c_2^1}, R_{c_2^1}, N_{c_2^2}, R_{c_2^2})$ and using eq. (3.6). With all these in mind, we have

	H_0	$-H_0$	H_1	$-H_1$	H_2	$-H_2$
$(v_f, v_{c_2^1}, v_{c_2^2})$	$(1,0,3)$	$(1,0,1)$	$(1,3,0)$	$(1,1,0)$	$(1,0,3)$	$(1,0,1)$

(4.11)

where $(v_f, v_{c_2^1}, v_{c_2^2})$ represents $(Z_f, 2\,\mathrm{Arg}[Z^R_{c_2^1}]/\pi, 2\,\mathrm{Arg}[Z^R_{c_2^2}]/\pi)$. We can evaluate $Z^R_{c_2^1}$ and $Z^R_{c_2^2}$ by the definition (1.5) as well, which will arrive at the same results as those in the above table.

4.3 Example: translation symmetry $j \to j+4$

For the systems with $U(1)+R$ symmetry and the translation symmetry: $j \to j+4$, there are two choices of reflection centers, as $\{c_4^1, c_4^3\}$ and $\{c_4^2, c_4^4\}$ shown in Fig 4.3, so the topology here is determined by which two kinds of reflection symmetries are preserved. For H_{int_0} and H_{int_2}, the only possible reflection centers are $\{c_4^1, c_4^3\}$, which are the same as $\{c^1, c^2\}$ in Fig 3.5 if we suppose the system in Fig 3.5 respects translation symmetry.

doi:10.6342/NTU202400302

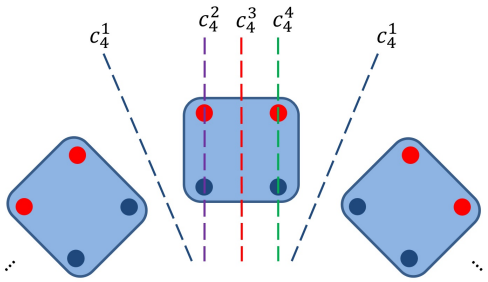

Figure 4.3: For the systems with $U(1)+R$ and the translation symmetry: $j \to j+4$, the reflection centers can be chosen as $\{c_4^1, c_4^3\}$ or $\{c_4^2, c_4^4\}$, depending on the system respects what kinds of reflection symmetry.

By use of Table 3.2 and eq. (3.6), we get

	H_{int_0}	$-H_{int_0}$	H_{int_2}	$-H_{int_2}$
$(v_f, v_{c_4^1}, v_{c_4^3})$	$(2,0,0)$	$(2,0,2)$	$(2,0,0)$	$(2,2,0)$

(4.12)

with $(v_f, v_{c_4^1}, v_{c_4^3}) = (Z_f, 2\,\mathrm{Arg}[Z^R_{c_4^1}]/\pi,\ 2\,\mathrm{Arg}[Z^R_{c_4^3}]/\pi)$. H_0, H_1, and H_2 also respect this translation symmetry, where the reflection centers can be $\{c_4^1, c_4^3\}$ or $\{c_4^2, c_4^4\}$. For the choice $\{c_4^1, c_4^3\}$, the corresponding topological invariants of these three systems are given by

	H_0	$-H_0$	H_1	$-H_1$	H_2	$-H_2$
$(v_f, v_{c_4^1}, v_{c_4^3})$	$(2,0,0)$	$(2,0,0)$	$(2,3,3)$	$(2,1,1)$	$(2,0,0)$	$(2,0,0)$

(4.13)

The topological invariants can be evaluated by definition or determined by the quantum number $(N_{c_4^1}, R_{c_4^1}, N_{c_4^3}, R_{c_4^3})$ of these decomposable systems. Here, we should be careful when assigning the quantum number to H_0 and H_2. Taking H_2 as an example, the picture

doi:10.6342/NTU202400302

of its charges in a subsystem is

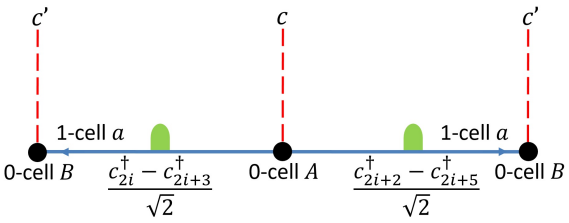

(4.14)

At first sight, one may think the corresponding quantum number is $(0,0,0,0)$. If we only want to know the information about $Z^R_{c^1_4}$ and $Z^R_{c^3_4}$, this quantum number is fine, but now we need all the information including Z_f, so it doesn't work, and we need a quantum number that satisfies the restriction (4.7). The valid quantum number can be obtained by moving charges while preserving reflection and translation symmetry, such as

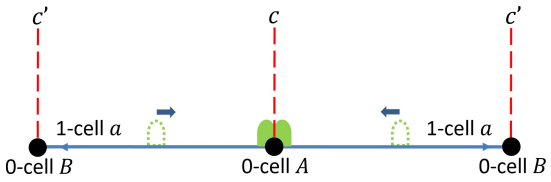

(4.15)

Since the reflection center is located between c_{2i+2} and c_{2i+3}, we have $R(c^\dagger_{2i}-c^\dagger_{2i+3})(c^\dagger_{2i+2}-c^\dagger_{2i+5})R^{-1} = (c^\dagger_{2i+5} - c^\dagger_{2i+2})(c^\dagger_{2i+3} - c^\dagger_{2i}) = -(c^\dagger_{2i} - c^\dagger_{2i+3})(c^\dagger_{2i+2} - c^\dagger_{2i+5})$, and hence the quantum number is $(2,1,0,0)$. We also can move charges to another reflection center (0-cell B), and the quantum number becomes $(0,0,2,1)$. Note that $(2,1,0,0)$ and $(0,0,2,1)$ are topologically identical because $(N_c, R_c, N_{c'}, R_{c'}) + n(2,1,-2,1) \sim (N_c, R_c, N_{c'}, R_{c'})$ where n is an integer. As a result, for H_2, the valid quantum number is $(0,0,2,1)$ or $(2,1,0,0)$ instead of $(0,0,0,0)$ because $(0,0,0,0)$ doesn't provide the right information about $\mathbb{Z}$ and therefore it can not describe $\mathbb{Z}\times\mathbb{Z}_2\times\mathbb{Z}_4$ classification. The above discussion is supported by the energy spectrum of $H_2 \to H_{int_2}$ shown in Fig 4.4, which indicates that H_2 and H_{int_2} are topologically identical. The quantum number of H_{int_2} is $(2,1,0,0)$, so $(0,0,0,0)$ cannot be the quantum number of H_2, otherwise, it will contradict the fact that

doi:10.6342/NTU202400302

$H_2 \sim H_{int_2}$.

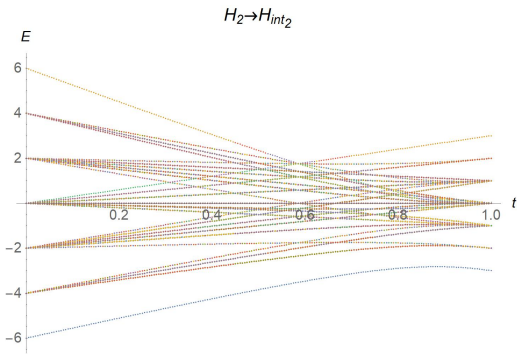

(a)

Figure 4.4: The eigenvalues of $H_2 \to H_{int_2}$ with PBC, where $N_{\text{tot}} = 12$. During the deformation, this system remains decomposable, so the energy gap is independent of N_{tot} and given by $E_1 - E_0$. Here, E_0 and E_1 are the energy of the ground state and the first excited state for a single subsystem.

doi:10.6342/NTU202400302

Chapter 5

Conclusion and Discussion

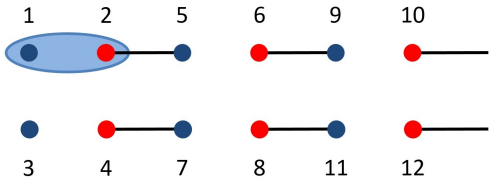

Figure 5.1: After rearranging, H_2 seems like stacking two dimerized SSH chains H_1.

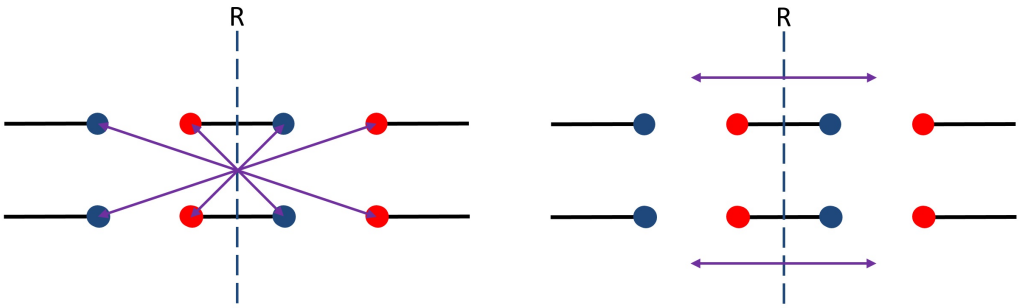

Figure 5.2: The purple arrows represent the directions of reflection symmetry. (a) The reflection symmetry of H_2. (b) The reflection symmetry of stacking two H_1.

We established the relation between decomposable systems and many-body topological invariants to physically realize two different kinds of SPT phases. For (1+1)d fermionic systems with $U(1) + S$ symmetry, by generalizing the idea of bulk-boundary correspondence from their free fermion counterparts in real space, we indicated the relation between $N_b - N_a$, which is a quantum number assigned to the decomposable systems that respect $U(1) + S$ symmetry, and the topological invariant Z^S. For the SPT phases protected by $U(1) + R$ symmetry, with the physical meaning provided by AHSS, we pointed out the relation between (N_c, R_c), which serves as a quantum number of decomposable systems

doi:10.6342/NTU202400302

with $U(1) + R$ symmetry, and Z^R.

Furthermore, we studied how these two kinds of SPT phases change when involving translation symmetry. For the cases with $U(1) + S$ symmetry, translation symmetry plays no role. However, for systems with $U(1) + R$ symmetry, because there is an interplay between reflection symmetry and translation symmetry, the classification becomes $\mathbb{Z} \times \mathbb{Z}_2 \times \mathbb{Z}_4$. With the hint of AHSS, we proved that $(Z_f, 2\,\mathrm{Arg}[Z_c^R]/\pi, 2\,\mathrm{Arg}[Z_{c'}^R]/\pi)$ is sufficient to be the set of topological invariants for this $\mathbb{Z} \times \mathbb{Z}_2 \times \mathbb{Z}_4$ classification.

On the other hand, although the consistency between phase transition points and energy gap closing points should be studied in the thermodynamic limit, we indicated this trait may appear when considering finite many-body systems with PBCs. Even though we only focused on two different kinds of SPT phases, the arguments regarding finite system energy spectrum should be applicable to other kinds of SPT phases because we didn't suppose any prerequisite here.

Finally, we want to point out one thing that may mislead people. After rearranging the unit cells as shown in Fig 5.1, the lattice model H_2 can be regarded as stacking two dimerized SSH chains H_1. But note that it only makes sense for cases with internal symmetries. When it comes to spatial symmetries, this idea doesn't work. Taking our cases as examples, we can see the discrepancy between H_2 and stacking two H_1 as shown in Fig 5.2.

doi:10.6342/NTU202400302

Appendix A — AHSS in generalized homology

For interacting systems, the classification of degree n SPT phenomena with crystalline symmetry G can be determined by the generalized homology $h_n^G(X,Y)$ where X and Y are real space and $Y \subset X$. In general, $h_n^G(X,Y)$ is quite difficult to compute, so we use the AHSS to simplify the computation [17]. The way AHSS is utilized to reach $h_n^G(X,Y)$ is as follows. We first take the G-symmetric cell decomposition of the space manifold X and then define the p-skeleton X_p of X

$$X_0 = \{0\text{-cells}\}, \qquad X_p = X_{p-1} \cup \{p\text{-cells}\}. \tag{A.1}$$

p-cell is a p-dimensional open cell in the cell decomposition. eq. (A.1) also implies the following relation

$$X_0 \subset X_1 \subset ... \subset X_d = X, \tag{A.2}$$

where d is the dimension of X. To proceed, we introduce the filtration of $h_n^G(X,Y)$

$$F_p h_n := \mathrm{Im}[h_n^G(X_p, X_p \cap Y) \to h_n^G(X,Y)]. \tag{A.3}$$

$F_p h_n$ can be regarded as the SPT phases on X by embedding the SPT phases on X_p into X. Due to eq. (A.2), we have

doi:10.6342/NTU202400302

$$0 \subset F_0 h_n \subset ... \subset F_d h_n = h_n^G(X, Y). \tag{A.4}$$

Combining eq. (A.4) and this relation $E^{\infty}_{p,n-p} \cong F_p h_n / F_{p-1} h_n$, we can get a series of short exact sequences:

$$\begin{aligned}
0 \to \ & E^{\infty}_{0,n} \ \to \ F_1 h_n \ \to E^{\infty}_{1,n-1} \to 0, \\
0 \to \ & F_1 h_n \ \to \ F_2 h_n \ \to E^{\infty}_{2,n-2} \to 0, \\
& \vdots \\
0 \to & F_{d-1} h_n \to h_n^G(X, Y) \to E^{\infty}_{d,n-d} \to 0.
\end{aligned} \tag{A.5}$$

$E^{\infty}_{p,n-p}$ is called the limiting page, which represents the $(n-p)$ dimensional SPT phases on p-cells that create no anomaly on any adjacent low-dimensional cells and cannot be trivialized by any adjacent high-dimensional cells. Here, if an SPT state on p-cells can be trivialized by an adjacent high-dimensional cell, it means that this SPT state can be created by adiabatically pumping the SPT states in this adjacent high-dimensional cell. Note that for a d-dimensional space manifold, the limiting page E^{∞} is the same as the converged page $E^{d+1}_{p,n-p}$. Using the above relation eq. (A.5) and given E^{∞}, we can obtain $h_n^G(X, Y)$ and each $F_p h_n$ by the iterative method.

Now, the last problem is how to get the E^{∞}-page. To address this problem, we start with the definition of E^1-page. For each p-cell D^p_j, there is a little group $G_{D^p_j} \subset G$ acts on D^p_j as on-site symmetry, so the cell decomposition leads to the "local data of SPT phases on D^p_j", $h^{G_{D^p_j}}_{p-q}(D^p_j, \partial D^p_j)$. If we consider the collection of these local data, we can define

doi:10.6342/NTU202400302

the E^1-page

$$E^1_{p,-q} = \prod_j h^{G_{D^p_j}}_{p-q}(D^p_j, \partial D^p_j), \tag{A.6}$$

where q is defined by $n = p - q$, and j runs the set of inequivalent p-cells of X. Because of bulk-boundary correspondence [47], it's reasonable to introduce the first differential (boundary map)

$$d^1_{p,-q} : E^1_{p,-q} \to E^1_{p-1,-q}. \tag{A.7}$$

Given that $E^1_{p,-q}$ can also be interpreted as degree $(n+1)$ anomalies, $d^1_{p,-q}$ is a map from the degree n (bulk) SPT phases on p-cells to the degree n (boundary) anomalies on adjacent $(p-1)$-cells. Owing to the fact that the boundary of the boundary is empty, $d^1_{p,-q} \circ d^1_{p+1,-q} = 0$, we can take the homology of d^1, which is defined as E^2-page

$$E^2_{p,-q} := \text{Ker}(d^1_{p,-q})/\text{Im}(d^1_{p+1,-q}). \tag{A.8}$$

Physically, $\text{Ker}(d^1_{p,-q})$ relates the degree n SPT states on p-cells that create no anomaly on adjacent $(p-1)$-cells, and $\text{Im}(d^1_{p+1,-q})$ denotes the degree n SPT states on p-cells that can be constructed by adiabatically pumping the SPT states in adjacent $(p+1)$-cells. Thus, $E^2_{p,-q}$ is a set of degree n SPT states on p-cells that can extend to adjacent $(p-1)$-cells without anomaly and cannot be trivialized by the SPT states in adjacent $(p+1)$-cells. Likewise, we can formulate the higher differential and E^r-page

$$\begin{aligned} d^r_{p,-q} &: E^r_{p,-q} \to E^r_{p-r,-q+r-1}, \\ E^{r+1}_{p,-q} &:= \text{Ker}(d^r_{p,-q})/\text{Im}(d^r_{p+r,-q-r+1}). \end{aligned} \tag{A.9}$$

$d^r_{p,-q}$ is called the r-th differential. Note that $E^{r+1}_{p,-q}$ is established because the relation

doi:10.6342/NTU202400302

$d^r_{p,-q} \circ d^r_{p+r,-q-r+1} = 0$ holds. In general, for a given E^1-page, we can get all E^r-pages up to the limiting pages by using eq. (A.9).

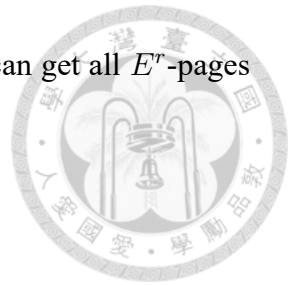

doi:10.6342/NTU202400302

Appendix B — Analytical calculations of $Z^R(H_1)$

In this section, we would like to show how to evaluate $Z^R(H_1)$ analytically. From eq. (3.8) and eq. (3.9), we have

$$[U_\alpha R]_I \left|GS(H_1)\right\rangle = \frac{1}{2^{(L+1)/2}}[\ldots(c_{2N}^\dagger - ic_{2M}^\dagger)A_{\text{part}}(ic_{2N+1}^\dagger - c_{2M+1}^\dagger)\ldots]\left|0\right\rangle, \quad \text{(B.10)}$$

where we choose $I = \{c_{2N+1}, \ldots, c_{2M}\}$ and

$$\begin{aligned} A_{\text{part}} &= i^{(N_\text{p}-1)}(c_{2M-1}^\dagger - c_{2M-2}^\dagger)\ldots(c_{2N+3}^\dagger - c_{2N+2}^\dagger) \\ &= i^{(N_\text{p}-1)}(-1)^{\sum_{j=1}^{N_\text{p}-1}(j-1)}(c_{2N+3}^\dagger - c_{2N+2}^\dagger)\ldots(c_{2M-1}^\dagger - c_{2M-2}^\dagger) \\ &= i^{(N_\text{p}-1)}(-1)^{(N_\text{p}-1)(N_\text{p}-2)/2}(-1)^{(N_\text{p}-1)}(c_{2N+2}^\dagger - c_{2N+3}^\dagger)\ldots(c_{2M-2}^\dagger - c_{2M-1}^\dagger), \end{aligned} \quad \text{(B.11)}$$

with $N_\text{p} = M - N$. It's straightforward to see that

$$\begin{aligned} Z^R(H_1) &= \left\langle GS(H_1)\right| [U_\alpha R]_I \left|GS(H_1)\right\rangle \\ &= \frac{2^{(L-1)/2}}{2^{(L+1)/2}}(-1)^{(N_\text{p}-1)(N_\text{p}-2)/2}(-1)^{(N_\text{p}-1)}i^{(N_\text{p}-1)}B_{\text{part}} \\ &= \frac{i^{(N_\text{p}-1)}}{4}(-1)^{(N_\text{p}-1)(N_\text{p}-2)/2}(-1)^{(N_\text{p}-1)}(1-i^2) \\ &= \frac{i^{(N_\text{p}-1)}}{2}(-1)^{(N_\text{p}-1)(N_\text{p}-2)/2}(-1)^{(N_\text{p}-1)}. \end{aligned} \quad \text{(B.12)}$$

Here $B_{\text{part}} = \left\langle 0\right| (c_{2M} - c_{2M+1})(c_{2N} - c_{2N+1})(c_{2N}^\dagger - ic_{2M}^\dagger)(ic_{2N+1}^\dagger - c_{2M+1}^\dagger)\left|0\right\rangle$.

doi:10.6342/NTU202400302

Appendix C — $(Z_f, 2\,\mathbf{Arg}[Z_c^R]/\pi, 2\,\mathbf{Arg}[Z_{c'}^R]/\pi)$ of generators

Considering the restriction (4.7), eq. (3.6), and the fact that $(N_c, R_c, N_{c'}, R_{c'}) + n(2, 1, -2, 1) \sim (N_c, R_c, N_{c'}, R_{c'})$ where n is an integer, $(Z_f, 2\,\text{Arg}[Z_c^R]/\pi, 2\,\text{Arg}[Z_{c'}^R]/\pi)$ of the generators in eq. (4.9) can be easily computed. As a reminder, Z_c^R and $Z_{c'}^R$ are determined by (N_c, R_c) and $(N_{c'}, R_{c'})$ separately, such as

$$(\underbrace{N_c, R_c}_{Z_c^R}, \underbrace{N_{c'}, R_{c'}}_{Z_{c'}^R}). \tag{C.13}$$

For $g_{\mathbb{Z}} = (1, 0, 0, 0)$, we have

$$\begin{aligned} &Z_f(H(ng_{\mathbb{Z}})) = n, \\ &2\,\text{Arg}[Z_c^R H(ng_{\mathbb{Z}})]/\pi = n \bmod 4, \\ &2\,\text{Arg}[Z_{c'}^R H(ng_{\mathbb{Z}})]/\pi = 0, \end{aligned} \tag{C.14}$$

where n is an integer, and $H(ng) = \bigoplus_{i=1}^{n} H(g)$. The above equation indicates

$$(v_f(H(ng_{\mathbb{Z}}), v_c(H(ng_{\mathbb{Z}}), v_{c'}(H(ng_{\mathbb{Z}})) = (n, n \bmod 4, 0) \in \mathbb{Z}, \tag{C.15}$$

with $(v_f, v_c, v_{c'}) = (Z_f, 2\,\text{Arg}[Z_c^R]/\pi, 2\,\text{Arg}[Z_{c'}^R]/\pi)$. For $g_{\mathbb{Z}_2} = (0, 1, 0, 0)$, we can get

doi:10.6342/NTU202400302

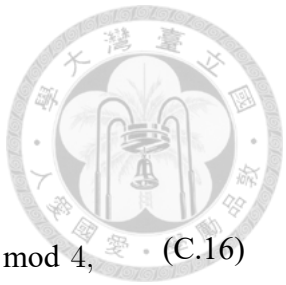

$$
\begin{aligned}
&Z_f(H(ng_{\mathbb{Z}_2})) = 0,\\
&2\,\mathrm{Arg}[Z_c^R H(ng_{\mathbb{Z}_2})]/\pi \sim 2\,\mathrm{Arg}[Z_c^R H(n(2,0,-2,1))]/\pi = 2n \bmod 4,\\
&2\,\mathrm{Arg}[Z_{c'}^R H(ng_{\mathbb{Z}_2})]/\pi = 0,
\end{aligned}
\tag{C.16}
$$

which leads to

$$
(v_f(H(ng_{\mathbb{Z}_2}), v_c(H(ng_{\mathbb{Z}_2}), v_{c'}(H(ng_{\mathbb{Z}_2})) = (0, n \bmod 2, 0) \in \mathbb{Z}_2. \tag{C.17}
$$

For $g_{\mathbb{Z}_4} = (1,0,-1,0)$, the values are given by

$$
\begin{aligned}
&Z_f(H(ng_{\mathbb{Z}_4})) = 0,\\
&2\,\mathrm{Arg}[Z_c^R H(ng_{\mathbb{Z}_4})]/\pi = n \bmod 4,\\
&2\,\mathrm{Arg}[Z_{c'}^R H(ng_{\mathbb{Z}_4})]/\pi \sim 2\,\mathrm{Arg}[Z_{c'}^R H(n(-3,0,3,0))]/\pi = 3n \bmod 4.
\end{aligned}
\tag{C.18}
$$

The equivalence classes of $(0, n \bmod 4, 3n \bmod 4)$ can be written as $[(0,0,0)]$, $[(0,1,3)]$, $[(0,2,2)]$, and $[(0,3,1)]$, so

$$
(v_f(H(ng_{\mathbb{Z}_4}), v_c(H(ng_{\mathbb{Z}_4}), v_{c'}(H(ng_{\mathbb{Z}_4})) = (0, n \bmod 4, 3n \bmod 4) \in \mathbb{Z}_4. \tag{C.19}
$$

doi:10.6342/NTU202400302

References

[1] Zheng-Cheng Gu and Xiao-Gang Wen. Tensor-entanglement-filtering renormalization approach and symmetry-protected topological order. Phys. Rev. B, 80:155131, Oct 2009.

[2] Xiao-Gang Wen. Symmetry-protected topological phases in noninteracting fermion systems. Phys. Rev. B, 85:085103, Feb 2012.

[3] Andrew M. Essin and Michael Hermele. Classifying fractionalization: Symmetry classification of gapped F_2 spin liquids in two dimensions. Phys. Rev. B, 87:104406, Mar 2013.

[4] Andrej Mesaros and Ying Ran. Classification of symmetry enriched topological phases with exactly solvable models. Phys. Rev. B, 87:155115, Apr 2013.

[5] Andreas P. Schnyder, Shinsei Ryu, Akira Furusaki, and Andreas W. W. Ludwig. Classification of topological insulators and superconductors in three spatial dimensions. Phys. Rev. B, 78:195125, Nov 2008.

[6] Giuseppe De Nittis and Kiyonori Gomi. Classification of "Quaternionic" Bloch-Bundles: Topological Quantum Systems of Type AII. Commun. Math. Phys., 339(1):1–55, 2015.

[7] Alexei Kitaev. Periodic table for topological insulators and superconductors. AIP Conference Proceedings, 1134(1):22–30, 05 2009.

doi:10.6342/NTU202400302

[8] Shinsei Ryu, Andreas P Schnyder, Akira Furusaki, and Andreas W W Ludwig. Topological insulators and superconductors: tenfold way and dimensional hierarchy. New Journal of Physics, 12(6):065010, jun 2010.

[9] Daniel S. Freed and Gregory W. Moore. Twisted Equivariant Matter. Annales Henri Poincaré, 12 2013.

[10] Guo Chuan Thiang. On the K-Theoretic Classification of Topological Phases of Matter. Annales Henri Poincaré, 04 2016.

[11] Ken Shiozaki, Masatoshi Sato, and Kiyonori Gomi. Atiyah-hirzebruch spectral sequence in band topology: General formalism and topological invariants for 230 space groups. Phys. Rev. B, 106:165103, Oct 2022.

[12] Xie Chen, Zheng-Cheng Gu, and Xiao-Gang Wen. Local unitary transformation, long-range quantum entanglement, wave function renormalization, and topological order. Phys. Rev. B, 82:155138, Oct 2010.

[13] Xie Chen, Zheng-Cheng Gu, Zheng-Xin Liu, and Xiao-Gang Wen. Symmetry protected topological orders and the group cohomology of their symmetry group. Phys. Rev. B, 87:155114, Apr 2013.

[14] Zheng-Cheng Gu and Xiao-Gang Wen. Symmetry-protected topological orders for interacting fermions: Fermionic topological nonlinear σ models and a special group supercohomology theory. Phys. Rev. B, 90:115141, Sep 2014.

[15] Ryan Thorngren and Dominic V. Else. Gauging spatial symmetries and the classification of topological crystalline phases. Phys. Rev. X, 8:011040, Mar 2018.

doi:10.6342/NTU202400302

[16] Hao Song, Sheng-Jie Huang, Liang Fu, and Michael Hermele. Topological phases protected by point group symmetry. Phys. Rev. X, 7:011020, Feb 2017.

[17] Ken Shiozaki, Charles Zhaoxi Xiong, and Kiyonori Gomi. Generalized homology and Atiyah-Hirzebruch spectral sequence in crystalline symmetry protected topological phenomena. Progress of Theoretical and Experimental Physics, page ptad086, 07 2023.

[18] Daniel S Freed and Michael J Hopkins. Reflection positivity and invertible topological phases. Geometry & Topology, 25:1165–1330, may 2021.

[19] Anton Kapustin. Symmetry protected topological phases, anomalies, and cobordisms: Beyond group cohomology, 2014.

[20] Anton Kapustin, Ryan Thorngren, Alex Turzillo, and Zitao Wang. Fermionic symmetry protected topological phases and cobordisms. Journal of High Energy Physics, 12 2015.

[21] Kazuya Yonekura. On the Cobordism Classification of Symmetry Protected Topological Phases. Communications in Mathematical Physics, 06 2019.

[22] Hassan Shapourian, Ken Shiozaki, and Shinsei Ryu. Many-body topological invariants for fermionic symmetry-protected topological phases. Phys. Rev. Lett., 118:216402, May 2017.

[23] Ken Shiozaki, Hassan Shapourian, and Shinsei Ryu. Many-body topological invariants in fermionic symmetry-protected topological phases: Cases of point group symmetries. Phys. Rev. B, 95:205139, May 2017.

[24] Ken Shiozaki, Hassan Shapourian, Kiyonori Gomi, and Shinsei Ryu. Many-body

doi:10.6342/NTU202400302

topological invariants for fermionic short-range entangled topological phases protected by antiunitary symmetries. Phys. Rev. B, 98:035151, Jul 2018.

[25] Ching-Kai Chiu, Jeffrey C. Y. Teo, Andreas P. Schnyder, and Shinsei Ryu. Classification of topological quantum matter with symmetries. Rev. Mod. Phys., 88:035005, Aug 2016.

[26] Xiao-Liang Qi, Hosho Katsura, and Andreas W. W. Ludwig. General relationship between the entanglement spectrum and the edge state spectrum of topological quantum states. Phys. Rev. Lett., 108:196402, May 2012.

[27] Xiao-Liang Qi and Shou-Cheng Zhang. Topological insulators and superconductors. Rev. Mod. Phys., 83:1057–1110, Oct 2011.

[28] M. Z. Hasan and C. L. Kane. Colloquium: Topological insulators. Rev. Mod. Phys., 82:3045–3067, Nov 2010.

[29] C. L. Kane and E. J. Mele. Z_2 topological order and the quantum spin hall effect. Phys. Rev. Lett., 95:146802, Sep 2005.

[30] Xiao-Liang Qi, Taylor L. Hughes, and Shou-Cheng Zhang. Topological field theory of time-reversal invariant insulators. Phys. Rev. B, 78:195424, Nov 2008.

[31] Cenke Xu and J. E. Moore. Stability of the quantum spin hall effect: Effects of interactions, disorder, and Z_2 topology. Phys. Rev. B, 73:045322, Jan 2006.

[32] Liang Fu, C. L. Kane, and E. J. Mele. Topological insulators in three dimensions. Phys. Rev. Lett., 98:106803, Mar 2007.

[33] Shinsei Ryu and Yasuhiro Hatsugai. Topological origin of zero-energy edge states in particle-hole symmetric systems. Phys. Rev. Lett., 89:077002, Jul 2002.

doi:10.6342/NTU202400302

[34] Hui Li and F. D. M. Haldane. Entanglement spectrum as a generalization of entanglement entropy: Identification of topological order in non-abelian fractional quantum hall effect states. Phys. Rev. Lett., 101:010504, Jul 2008.

[35] Y. Hatsugai. Bulk-edge correspondence in graphene with/without magnetic field: Chiral symmetry, dirac fermions and edge states. Solid State Communications, 149(27):1061–1067, 2009.

[36] P. Delplace, D. Ullmo, and G. Montambaux. Zak phase and the existence of edge states in graphene. Phys. Rev. B, 84:195452, Nov 2011.

[37] Roger S. K. Mong and Vasudha Shivamoggi. Edge states and the bulk-boundary correspondence in dirac hamiltonians. Phys. Rev. B, 83:125109, Mar 2011.

[38] Gian Michele Graf and Marcello Porta. Bulk-edge correspondence for two-dimensional topological insulators. Communications in Mathematical Physics, 324(3):851–895, October 2013.

[39] János K. Asbóth, László Oroszlány, and András Pályi. A Short Course on Topological Insulators. Springer International Publishing, 2016.

[40] Yang Peng, Yimu Bao, and Felix von Oppen. Boundary green functions of topological insulators and superconductors. Phys. Rev. B, 95:235143, Jun 2017.

[41] Chen-Shen Lee, Iao-Fai Io, and Hsien-chung Kao. Winding number and zak phase in multi-band ssh models. Chinese Journal of Physics, 78:96–110, August 2022.

[42] Lukasz Fidkowski and Alexei Kitaev. Effects of interactions on the topological classification of free fermion systems. Phys. Rev. B, 81:134509, Apr 2010.

doi:10.6342/NTU202400302

[43] Evelyn Tang and Xiao-Gang Wen. Interacting one-dimensional fermionic symmetry-protected topological phases. Phys. Rev. Lett., 109:096403, Aug 2012.

[44] Bo-Hung Chen and Dah-Wei Chiou. An elementary rigorous proof of bulk-boundary correspondence in the generalized su-schrieffer-heeger model. Physics Letters A, 384(7):126168, 2020.

[45] Chen-Shen Lee. A linear algebra-based approach to understanding the relation between the winding number and zero-energy edge states, 2023.

[46] Frank Pollmann, Ari M. Turner, Erez Berg, and Masaki Oshikawa. Entanglement spectrum of a topological phase in one dimension. Phys. Rev. B, 81:064439, Feb 2010.

[47] Xie Chen, F. J. Burnell, Ashvin Vishwanath, and Lukasz Fidkowski. Anomalous symmetry fractionalization and surface topological order. Phys. Rev. X, 5:041013, Oct 2015.

doi:10.6342/NTU202400302